Received: 30 July 2019 | Revised: 8 September 2019 | Accepted: 17 September 2019

DOI: 10.1002/inf2.12054

REVIEW ARTICLE

WILEY

3D electronic and photonic structures as active biological interfaces

Huachun Wang[1,2] | **Pengcheng Sun**[3] | **Lan Yin**[3] | **Xing Sheng**[1,2]

[1]Department of Electronic Engineering, Beijing National Research Center for Information Science and Technology, Tsinghua University, Beijing, China

[2]IDG/McGovern Institute for Brain Research, Tsinghua University, Beijing, China

[3]School of Materials Science and Engineering, Tsinghua University, Beijing, China

Correspondence
Lan Yin, School of Materials Science and Engineering, Tsinghua University, Beijing 100084, China.
Email: lanyin@mail.tsinghua.edu.cn

Xing Sheng, National Research Center for Information Science and Technology, Tsinghua University, Beijing 100084, China.
Email: xingsheng@tsinghua.edu.cn

Funding information
National Natural Science Foundation of China, Grant/Award Numbers: 61874064, 51601103; Key Laboratory of Advanced Materials of Ministry of Education of China, Grant/Award Number: XJCL201903; Beijing National Research Center for Information Science and Technology at Tsinghua University, Grant/Award Number: BNR2019ZS01005

Abstract

Biocompatible materials and structures with three-dimensional (3D) architectures establish an ideal platform for the integration of living cells and tissues, serving as desirable interfaces between biotic and abiotic systems. While conventional 3D bioscaffolds provide a mechanical support for biomatters, emerging developments of micro-, nano-, and mesoscale electronic and photonic devices offer new paradigms in analyzing and interrogating biosystems. In this review, we summarize recent advances in the development of 3D functional biointerfaces, with a particular focus on electrically and optically active materials, devices, and structures. We first give an overview of representative methods for manufacturing 3D biointegrated structures, such as chemical synthesis, microfabrication, mechanical assembly, and 3D printing. Subsequently, exemplary 3D nano-, micro-, and mesostructures based on various materials, including semiconductors, metals, and polymers are presented. Finally, we highlight the latest progress on versatile applications of such active 3D structures in the biomedical field, like cell culturing, biosignal sensing/modulation, and tissue regeneration. We believe future 3D micro-, nano-, and mesostructures that incorporate electrical and/or optical functionalities will not only profoundly advance the fundamental studies in biological sciences, but also create enormous opportunities for medical diagnostics and therapies.

KEYWORDS

3D structures, biointerfaces, electronics, photonics

1 | INTRODUCTION

Biological science that studies life and living organisms has become one of the emerging disciplines and is progressively actuated by its medical potential for resolving health issues and improving health care.[1,2] Investigations into the enormous biosystems, including their physical conformations, biochemical interactions, internal physiological mechanisms, and so on, not only provide opportunities to thoroughly understand lives from the scientific perspective, but also offer paths to novel technologies for biomedical diagnostics and therapies. Biointerfaces, which are defined as the interfaces between biological systems and synthetic materials,[3,4] act as an

interdisciplinary area to explore biological science and clinical applications. In past decades, micro-, nano-, and mesoscale structural biointerfaces have been designed and formed by transforming synthetic materials into various geometries, including zero-dimensional (0D),[5-7] one-dimensional (1D),[8-10] two-dimensional (2D),[11-13] and three-dimensional (3D) configurations.[14-17] Due to their cellular and subcellular size, low-dimensional (0D, 1D, and 2D) materials and structures present particular physical and chemical characters pertinent to biological systems, promoting their usages for revolutionary biological studies as functional biointerfaces.[18] For example, a recent work made an overview of 0D luminescent nanoparticles for tracking single molecules as well as imaging subcellular structures in living systems in real time.[19] In another thrust, photoelectrochemical modulations for neurons via freestanding silicon (Si) 1D nanowires were demonstrated.[20] Undoubtedly, strategies for biological manipulations based on these low-dimensional biointerfaces are promising for both fundamental and clinical applications. Nevertheless, biological systems, including molecules, cells, tissues, and organs, are naturally delicate, irregular, and inhomogeneous with complex anisotropic 3D structures embraced in stereoscopic environments. Consequently, low-dimensional biointerfaces with simple structures are incapable of fully fulfilling realistic requirements for high-fidelity comprehension of the biological systems within in vitro and/or in vivo conditions. To adapt to the sophisticated 3D biological matters and overcome the deficiencies of low-dimensional structures, hierarchically configured 3D biointerfaces are actively exploited for ideal biointegration within in vitro and/or in vivo conditions.

In fact, biological scaffolds together with engineered 3D biointerfaces have been extensively studied and applied for tissue regeneration and remodeling engineering.[21] A representative example is the utilization of 3D bioscaffolds for bone tissue regeneration engineering.[22] During this regenerative process, 3D biointerfaces between the scaffolds and bone tissues play a pivotal role for cell attachment, proliferation, induced differentiation, and tissues regeneration with designate-oriented assembly.[23] Depending on targeted applications, these conventional 3D scaffolds can be based on certain metals (titanium alloys, stainless steels, etc.), synthetic polymers (polylactides, polycaprolactone, etc.), hydrogels, and hybrid materials.[24] With proper structural and mechanical properties, these scaffolds are able to resemble real tissues and provide topographic support for living cells in biosystems, exhibiting reasonable biocompatibility and even biodegradability. However, these scaffolds are limited to construct effective extracellular matrix (ECM) microenvironment and to meet clinical requirements. For this case, growth factors (physiologic polypeptides) are generically employed to improve bioactivity of the scaffolds via biomimetic ECM rebuilding.[25] Noteworthily, this incorporation creates vast complexity in practice and, even worse, causes functional decline of scaffolds because of the short-term, indirect biochemical interaction with cells. Obviously, high-performance scaffolds are needed to furnish with bioactive cues to communicate with biosystems from their inherent mechanisms and connotation. It is clear that physical signals, especially electrical signals, are also the basis of biological activity and action, as well as the realization of fundamental functions of biosystems, ranging from molecules to whole organs.[26]

Physical biology built upon physical principles and methods imparts radical insight into the role of electrical biointerfaces to straightforwardly discover the underlying transduction mechanisms in the biological world. For example, electrophysiological techniques perform electronic sensing by converting biological signals (ions) into current or voltage, which have been widely utilized not only for cellular research (such as ion channel proteins) in laboratories, but also for disease treatment (such as heart arrhythmia) in clinical practice. Up to date, advanced electronics (typically miniaturized, physically transient, and soft 3D electronics) along with the formed electrical activated biointerfaces have been deeply developed as multifunctional platforms for a broad spectrum of application areas, reaching nearly every class of the hierarchical biosystems, including molecular detection and sensing,[27] cellular recording and stimulation,[28] and tissue regeneration and modulation.[29] In addition to electrical biointerfaces, optical biointerfaces resulting in physiological functions by photons known as biological fluorescence in early stage are also of growing interest owing to their potential applications in fields as diverse as molecular visually tracking,[19] neuroscience investigations,[30] and photodynamic therapy (PDT).[31] A breakthrough on optical biointerfaces is the advent of optogenetics that modulates neural activities with high spatiotemporal resolutions by expressing light-sensitive actuators and leads to precise causal manipulation of neural circuits,[32,33] concerning on neurological problems like Parkinson's disease, epilepsy, and blindness due to neuronal loss.[34,35] Taken together, compared to conventional biochemical interface, either electrical or optical biointerfaces exhibit distinguished features of reliable, controllable, versatile, multiscale, and substantial biophysical interactions at high spatiotemporal resolutions, which open up opportunities for their biological applications, notably extending to human beings.

In this review, we focus on the recent new phenomena and developments of the state-of-the-art

nonconventional 3D multifunctional biointerfaces that are electrically and/or optically active. Discussions begin with diverse techniques as approaches to 3D manufacturing in advanced functional materials. Subsequently, we emphatically illustrate various types of biocompatible, multipurpose materials (semiconductors, carbon-based materials, metals, organic polymers, and hybrid materials, as summarized in Table 1) that display unique physical properties. Then, we highlight the 3D multifunctional biointerfaces, principally regarding bioelectronics and biophotonics interfaces for some leading biological applications such as cell culture, signal recording, behavior regulation, and therapy. Finally, we describe the challenges and opportunities, and conclude by outlining perspectives on future research.

TABLE 1 Summary of representative materials and methods to form functional, electrically, and/or optically active biostructures

Category	Materials	Manufacturing
Semiconductors	Si, InP, GaP, ZnO, GaN	Vapor-based deposition
		Mechanical buckling
		Microfabrication
		Printing-based assembly
Polymers	PEDOT:PSS, PPy, PANI	Microfabrication
		3D printing
		Electrospinning
		Salt-leaching
Metals	Au/Pt (SU-8/PDMS)	Microfabrication
		Elastocapillary
Carbon-based materials	Graphene, carbon nanotubes	Vapor-based deposition
		Physical exfoliation
Hybrid materials	Si/Au-PLGA/Alginate	Microfabrication
	PPy-PLGA/PCL	Printing-based assembly
		Salt-leaching

Abbreviations: 3D, three-dimensional; Au, gold; GaN, gallium nitride; GaP, gallium phosphide; InP, indium phosphide; PANI, polyaniline; PCL, polycaprolactone; PDMS, polydimethylsiloxane; PEDOT:PSS, poly(3,4-ethylenedioxythiophene):poly(styrenesulfonate); PLGA, poly(lactic-co-glycolide); PPy, polypyrrole; Pt, platinum; Si, silicon; ZnO, zinc oxide.

2 | METHODS

2.1 | Vapor-based deposition

Semiconductors display a wide range of controllable physical properties such as doping level, geometry, and composition, and thus could lead to tunable electrical and optical performance, which allows them to become versatile platforms for different biological applications. In the case of building functional semiconductors with complicated 3D geometries, vapor-liquid-solid (VLS) or vapor-solid (VS) methods have attracted significant attentions due to its simplicity and versatility. An up-to-date overview of research concerning VLS and VS is provided in details by Guniat et al.[36]

The VLS growth mechanism for semiconductor nanowires was first demonstrated in the work by Wagner and Ellis,[37] who recognized that the crystallization of silicon whiskers could be mediated by a liquid metal droplet at a lower temperature. Later findings also illustrated that crystallization of Si and germanium (Ge) have been succeeded by alloying gold (with Ge or Si) at a eutectic temperature as low as 360°C.[38] Taking Si as an example, silicon tetrachloride ($SiCl_4$), silane (SiH_4), or pure Si is fed into a chamber as the vapor phase precursors. As the precursors decompose and penetrate into the gold (Au) surfaces, then the Si-Au alloy droplets can be formed at a temperature below pyrolysis of Si. Due to the supersaturation effect, Si atoms are able to precipitate from the bottom of alloy droplets and to eventually integrate into vertical nanowires. During this growth process, the locations and lateral sizes of the nanowire are well confined by the top liquid droplets. Obviously, metals or intermediate phases as catalyst are necessary to grow semiconductors for VLS method. Relatively, as an alternative catalyst-free path, the proposed VS method could eliminate the catalysts to grow semiconductors directly through the effect of imbalance in crystal growth velocities.[39] Semiconductors like gallium nitride (GaN) and indium arsenide (InAs) are typically prepared via VS method.

Additionally, one of the most attractive features of the VLS method is that semiconductors can be transformed into heterostructures and complex 3D structures (Figure 1A), which enable them to create new systems with fundamentally new characteristics and functionalities. Figure 1B shows a vertically oriented 3D Ge nanowire array grown from Au colloids on a Si substrate. Generally, a polyelectrolyte layer with positive charges on the substrate is used as a binder to link the negatively charged gold colloids. Here, a linker-free method is presented to deposit Au colloids onto hydrogen-terminated Si substrate by acidifying the Au colloids solution with hydrochloric acid or hydrofluoric acid, which could

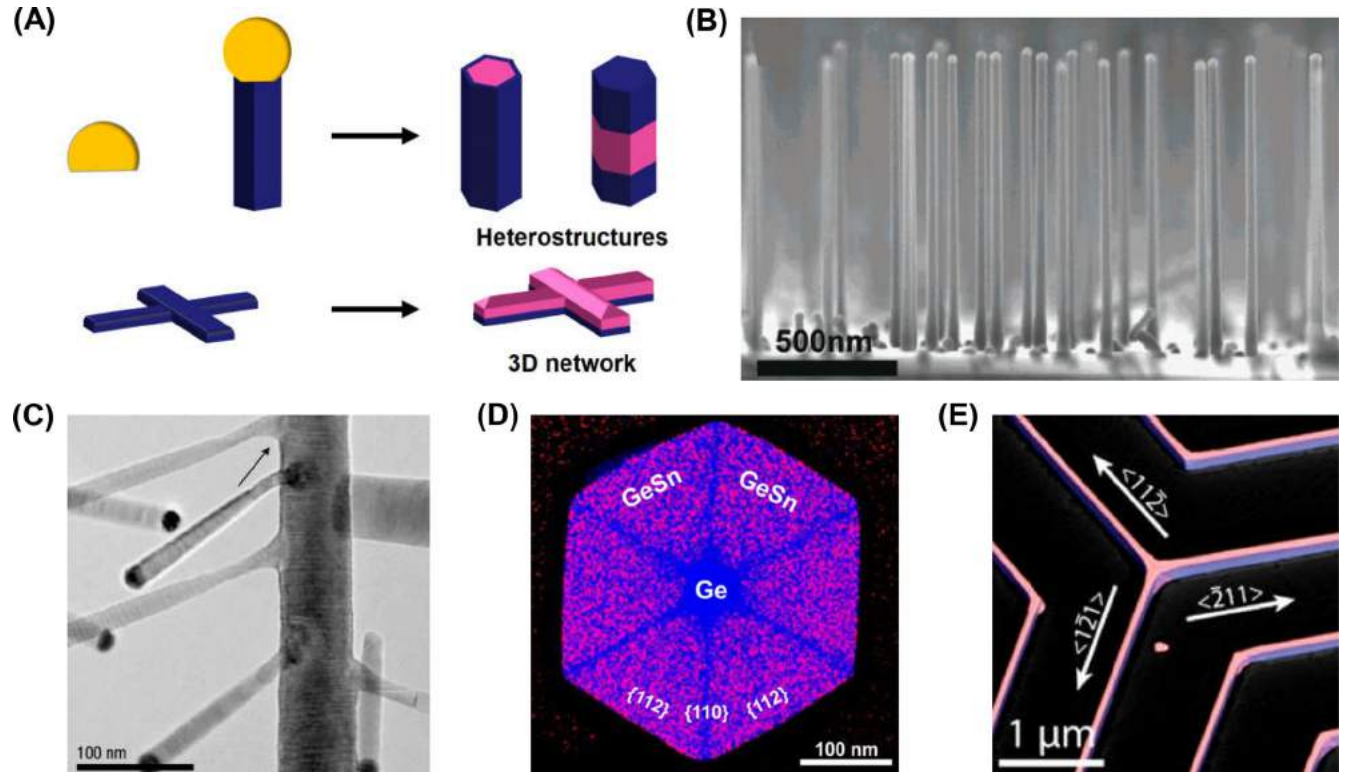

FIGURE 1 A, 3D structures and heterostructures using vapor-liquid-solid or vapor-solid growth. B, Vertical Ge nanowires array. Reproduced with permission.[40] Copyright 2007, American Chemical Society. C, Transmission electron microscope images of GaP nanotrees. Reproduced with permission.[41] Copyright 2004, Nature Publishing Group. D, Cross-sectional energy-dispersive X-ray spectroscopic (EDS) mapping of a Ge/GeSn core-shell nanowire. Reproduced with permission.[42] Copyright 2017, American Chemical Society. E, Scanning electron microscopy (SEM) image of a branched GaAs/InSn nanomembranes/nanowires network. Reproduced with permission.[43] Copyright 2018, American Chemical Society

prevent oxide formation during the epitaxial process of Ge nanowires.[40] In addition to the vertical Ge nanowires array, gallium phosphide (GaP) with tree-like nanostructures were further developed via the VLS growth process by Dick et al,[41] as showed in Figure 1C. The fabrication process contained two steps, the forming of trunk and the growth of branching structures. Because of their high surface area-to-volume ratio, these novel tree-like 3D nanostructures hold promising biological application as photoelectrochemical devices.[44] In addition to the innovation of geometrical structures, integration of multiple semiconductor materials has attracted further attention, as the well-known semiconductor heterostructures combining with particular optoelectronic properties. As demonstrated in Figure 1D, high-quality Ge/GeSn (germanium-tin) core/shell heterostructure nanowires arrays were synthesized via VLS at a low temperature (~300°C).[42] Besides, the GeSn alloys possessed a direct bandgap of about 0.465 eV, with the potential to form shortwave infrared detectors for biomedical spectrographic applications. Quite recently, InAs/gallium arsenide (GaAs) heterostructure-based nanowire networks in wafer scale were introduced by using the template-assisted selective area epitaxy growth.[43] As shown in Figure 1E, the researchers developed a gold-free fabrication process utilizing GaAs nanomembranes as templates for InAs nanowire growth. These emerging techniques provide inspiring strategies to assemble sophisticated semiconductor heterojunctions.

Besides, the vapor-based deposition is also utilized to grow 1D, 2D, and 3D carbon-based materials that hold great potential for biological investigation. For example, as a "bottom-up" approach to fabricate graphene, it involves active gaseous precursors (like methane, CH_4), specific substrates as catalysts (like copper and nickel), and suitable reaction temperature (~1000°C). Using the chemical vapor deposition (CVD) method, large area, either multilayer, or single-layer graphene can be obtained.

2.2 | Microfabrication and printing-based assembly

Lithographic tools are widely used to form patterned micro- and nanostructures in large-scale integrated

circuits. Furthermore, advanced assembly methods like wafer/chip bonding and transfer printing are developed to realize more versatile heterogeneous materials and device integration. For example, Kim et al[45] studied a microtransfer printing process to pattern gold electrodes on cellulose electroactive paper (EAPap) using polydimethylsiloxane (PDMS)-based stamps, aiming to develop biodegradable and flexible electronic circuits (Figure 2A). In this method, a separator was coated on the PDMS stamp and an adhesive membrane was coated on the cellulose paper to facilitate the transfer process.[52] Combining this approach with biomaterials can produce various integrated microprobes for health monitoring in human body. Lu et al[46] integrated a miniaturized light source and a photodetector on a biocompatible and flexible micro-needle-shaped polyimide chip (Figure 2B1), which could be inserted into the deep brain of mice and achieve long-term and stable detection of neuronal

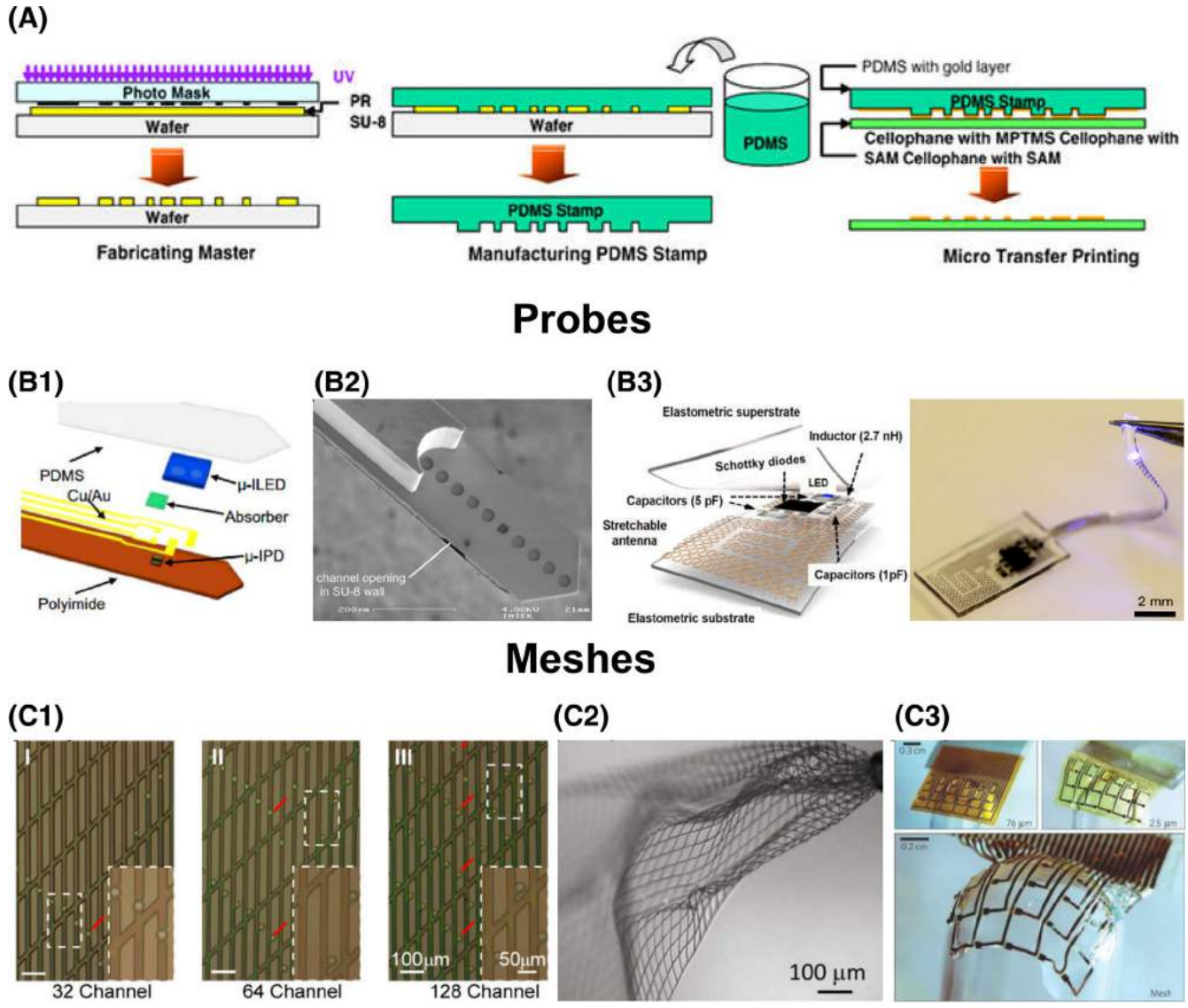

FIGURE 2 A, Process flow of microfabrication and transfer printing. Reproduced with permission.[45] Copyright 2006, IOP Publishing. B1, Schematic illustration of a wireless probe integrating a microscale inorganic light-emitting diode (μ-ILED) and a microscale inorganic photodetection (μ-IPD). Reproduced with permission.[46] Copyright 2018, PNAS. B2, Scanning electron microscope image of a probe showing the front side, electrode sites, square-shaped channel opening in the polyimide foil and lateral channel opening in the SU-8 channel wall. Reproduced with permission.[47] Copyright 2013, The Royal Society of Chemistry. B3, Schematic and photograph of an epidural probe, highlighting the soft, stretchable connection to an LED. Reproduced with permission.[48] Copyright 2015, Nature Publishing Group. C1, Microscope images of mesh electrodes. Insets: zoom-in views. Reproduced with permission.[49] Copyright 2017, PNAS. C2, Injection of mesh electronics into aqueous solution.[50] Reproduced with permission. Copyright 2015, Nature Publishing Group. C3, Images of electrode arrays wrapped onto a glass hemisphere. Reproduced with permission.[51] Copyright 2010, Nature Publishing Group

dynamics. Rubehn et al[47] fabricated a polymer-based shaft electrode (Figure 2B2) and integrated SU-8-based waveguide and fluidic channel into it by using microelectromechanical systems. With similar approaches, Sung et al[48] achieved a wireless, minimally invasive optoelectronic system (Figure 2B3) that interfaced with multiple neural cells. Furthermore, taking advantage of microfabrication and printing assembly, highly integrated, flexible, and multichannel electronics for stable chronic brain detection were fabricated, such as multichannel mesh electronics (Figure 2C1),[49] syringe-injectable electronics (Figure 2C2),[50] and silk-based ultrathin degradable electronics (Figure 2C3).[51] It can be seen from these examples that versatile micro- and nanofabrication techniques provide viable solutions to accurately and chronically operate 3D biological interfaces.

2.3 | Mechanical force-guided assembly

Recently, mechanical force-guided assembly becomes one of the most prevailing manners to construct nano-, micro-, and mesoscale 3D structures for its ability to form highly intricate and deterministic 3D configurations at a low cost and large scale. Typical mechanical driving

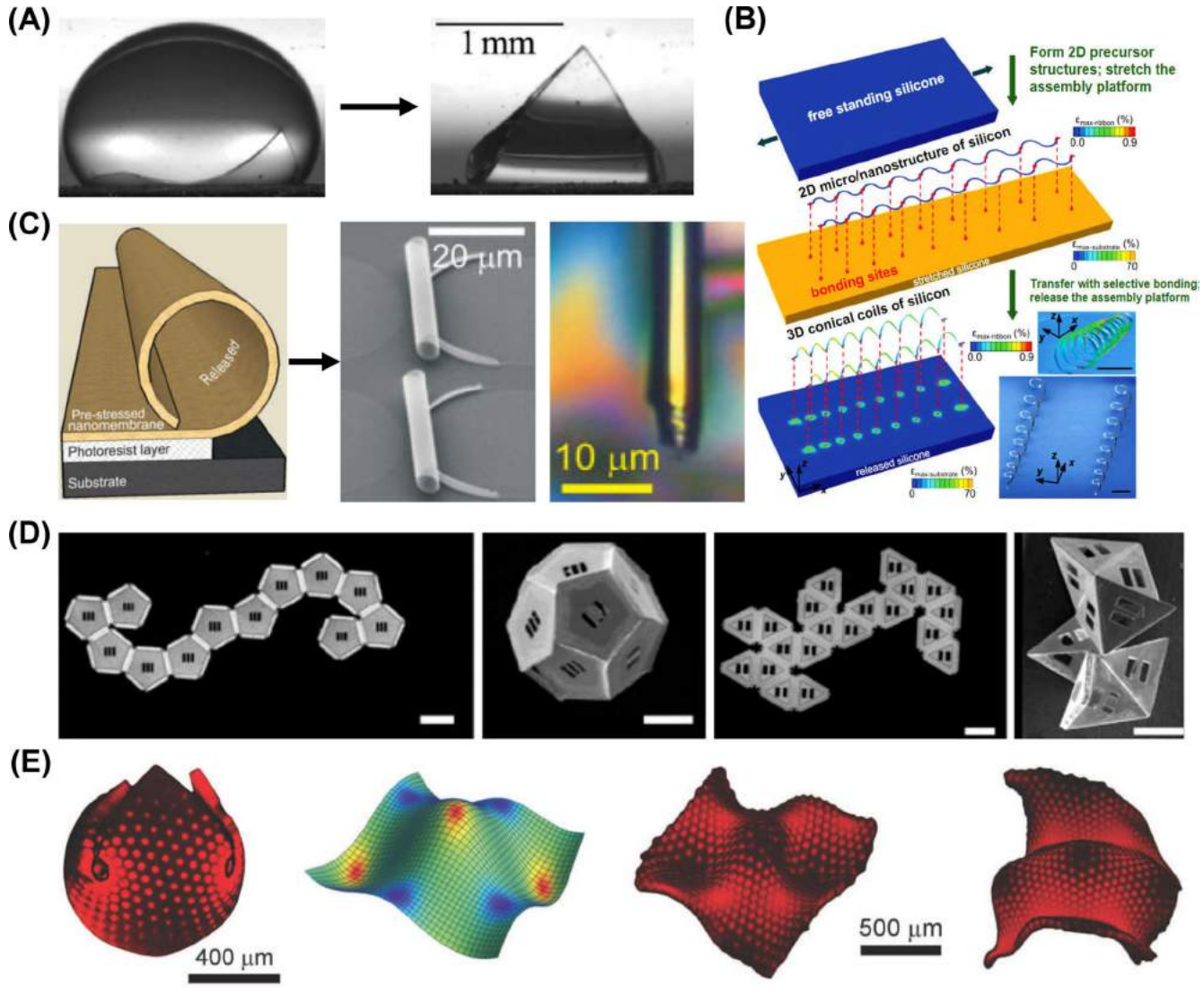

FIGURE 3 A, Transformation of a flat film to a triangular shape by capillary force. Reproduced with permission.[54] Copyright 2007, American Physical Society. B, Process for the deterministic assembly of 3D mesostructures made of monocrystalline silicon, scale bar 400 μm. Reproduced with permission.[55] Copyright 2015, AAAS. C, Illustration of rolling up a nanomembrane into a tube (left), scanning electron microscope image of Si/SiO_2 tubes, and optical image of Pd/Fe/Pd tube respectively (right). Reproduced with permission.[56] Copyright 2008, Wiley-VCH. D, Images of self-folding nets, dodecahedra (left) and icosahedra (right), scale bar 300 μm. Reproduced with permission.[57] Copyright 2011, PNAS. E, Designing responsive buckled surfaces by halftone gel lithography. Reproduced with permission.[58] Copyright 2012, AAAS

forces used to build structures include capillary forces, compressive forces, and residual stress.

Capillary actions result from the intermolecular attraction between liquid and solid, which can be utilized for advanced micro- and nanomanufacturing. The generated surface forces between the liquid and surrounding solid, known as capillary forces utilized to form 3D structures such as bundles, rackets, and folded films have been intensively studied in recent years.[53] Figure 3A illustrates the effect of capillary forces on a flat elastic PDMS membrane that led to a predetermined 3D shape.[54] This spontaneous folding process occurred in a time-lapse sequence as a liquid droplet deposited on a triangular PDMS membrane. The corners of the PDMS membrane would fold toward the center and the flat membrane turned into a tetrahedral pyramid along with the connected corners at the center. Along with further evaporation of the liquid droplet, buckling on the pyramid walls occurred due to the negative internal pressure. In such a capillary origami process, elastocapillary length determined the minimal folding size of a flat membrane.[59] By employing the capillary forces to assemble 3D electronic structures, Guo et al[60] exploited the 3D folding of single-crystalline silicon-based photovoltaic devices to improve the power conversion efficiency.

Compressive forces can also be applied to form sophisticated 3D geometrical structures such as multilevel and hierarchical mesostructures.[61] This process depends on the compressive forces exerting to an elastometric substrate to transform the prefabricated planar precursor structure into a 3D configuration through controlled compressive buckling with strain release. This original concept in assembling 3D architectures was presented by Xu and coworkers,[55] as showed in Figure 3B in details. The 2D precursors of planar serpentine silicon ribbons were first fabricated by micro/nanofabrication technologies. Afterward, accurately patterned structures of surface hydroxyl terminations at desired locations (red dots in Figure 3B) were produced lithographically by the exposure of ozone made using ultraviolet light. At the same time, the soft silicone elastomer substrate was stretched to a large level of prestrain and was then exposed to ozone to generate uniform coverage of surface hydroxyl groups serving as a platform that guided the mechanical assembly for silicon ribbons. After the aforementioned steps, the serpentine silicon ribbons were transferred onto the treated surface of the elastomer substrate. Accordingly, firm and spatially selective bonding was formed via covalent linkages of the hydroxyl groups between silicon ribbons and silicone substrate. As the substrate recovering to its original shape, the induced compressive forces would act on the serpentine precursors. Consequently, 3D helical silicon ribbons were achieved through the compressive force-guided assembly. This compressive force assembly has been further studied as a reliable method to establish highly complex multilevel or hierarchical 3D mesostructures.[62]

Residual stress-induced self-folding has been demonstrated as another effective force-based assembly approach, which is often used to form rolled tube structures driven by the minimization of surface tension. In early days, this strain engineering-based approach has limited applications because of strict requirements for various desirable materials. Figure 3C shows an improved method that can be applied for a broad range of materials and material combinations.[56] Inorganic nanomembranes deposited onto a photoresist-based sacrificial interlayer could be easily released from the substrate by removing the sacrificial layer with solvents like acetone and roll up into a 3D nanotube shape. By adopting this generic approach, various tubular micro or nanostructures based on different materials (Pt: platinum, TiAu: titanium gold, TiO_2: titanium dioxide, ZnO: zinc oxide, Si_xN_y: silicon nitrides, etc.) have been built with precisely controlled diameters and lengths. As an application of this technology, the rolled-up microtubes were used as bio-cell growth-guided scaffolds for cell culture. In addition, polyhedral structures driven by surface tension utilizing discrete geometry were designed and formed by Pandey et al[57] with both experimental and theoretical investigations. The authors discussed the criterion for the synthesis of polyhedra by self-folding using planar nets and found that compactness was an effective design criterion for high polyhedra, especially for truncated octahedron, dodecahedron and icosahedron, as shown in Figure 3D. These findings offered profound insight into self-assembly of complex 3D structures by designing computed configuration space and folding pathways.

Active materials that respond to certain stimuli such as heat and light are ideal for fabricating reversible 3D structures, holding promises in application areas such as bioelectronics, bionics, and biomedicine. For example, Kim and coworkers developed the temperature-responsive N-isopropylacrylamide (NIPAm) copolymer to form 3D geometries via a proposed method called "ehalftone gel lithography."[58] Such a technique utilized two photomasks to produce highly cross-linked dots embedded in the photo-cross-linkable NIPAm polymer film, and enabled the fabrication of stimulus-responsive gel patterned sheets, thereby leading to predictable 3D structures (Figure 3E).

2.4 | 3D printing

As a widely used additive manufacturing technique, 3D printing employs a layer-by-layer method to join specific materials to make objects from 3D models.[63] It enables to

fabricate large-scale, soft, and flexible bioelectronics at low cost.[64] As a typical example of 3D printing, direct ink writing employs a computer-controlled translation ink-deposition nozzle to create 3D models with designed architecture and composition.[65] The direct ink writing methods can be divided into inkjet-based approaches and extrusion-based approaches (Figure 4A, left). The inkjet printing is only appropriate for the materials within a very small viscosity range (about 10 times that of pure water), while extrusion printing squeezes materials out of a very thin nozzle by exerting high pressure to the injection head. Thus, various materials with a wide range of viscosity can be shaped with the extrusion printing (Figure 4A, left).[70] For example, quantum dot-based light-emitting diodes (QD-LEDs) with multiple active layers can be fabricated by using 3D extrusion printing (Figure 4A, right).[66] Multiple layers of materials were sequentially printed to form this device, including: (a) cadmium selenide/zinc sulfide (CdSe/ZnS) core-shell QDs as the emission layer, (b) poly(*N*,*N*′-bis (4butylphenyl)-*N*,*N*′-bis(phenyl)-benzidine) as the hole transport layer, (c) poly(ethylenedioxythiophene):polystyrene sulfonate (PEDOT:PSS) as the transparent anode, surrounded by (d) a sintered silver nanoparticle ring metallic interconnect, and (e) a eutectic gallium indium liquid metal cathode. Taking advantage of the ability of extrusion printing to print high viscosity inks, Ahn et al[67] proposed a method by using silver nanoparticle inks to form highly conductive cables with a high aspect ratio, and possibly spanning in 3D (Figure 4B).

Besides direct ink writing, a novel 3D printing method based on optical projection was introduced for additive manufacturing. In such a method, an oxygen "dead zone" was developed by using an oxygen-permeable window based on amorphous fluoropolymer between the ultraviolet image projection plane and the liquid precursor (Figure 4C).[68] In this zone, photopolymerization was prevented and both of the continuity and fineness could be greatly improved for the printed structures. On 2D planes, printers are able to form conductive polymer[71,72] and inorganic semiconductor,[73] and 3D printing is mostly composed of 2D plane splicing into 3D structure, which greatly reduces the continuity of the final product. Kelly et al[69] were inspired by computed tomography, a nondestructive imaging technique widely used in the medical field,[74,75] and designed a new 3D printing method by utilizing tomographic reconstruction technology (Figure 4D). The 3D object was decomposed into 2D patterns with different angles, and these patterns were projected into the photosensitive liquid from different angles by light, so as to form complete 3D patterns without considering support structures. The 3D printing

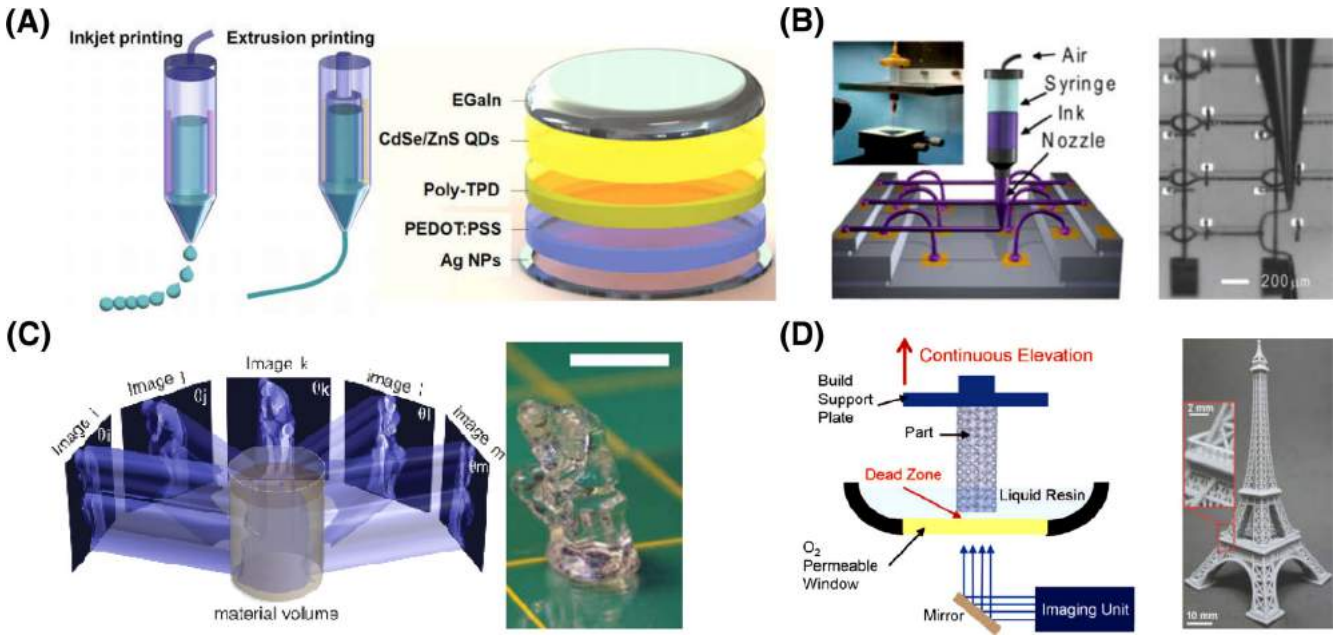

FIGURE 4 A, Schematic diagrams of 3D-inject printing and 3D-extrusion printing (left) and directly 3D printed QD-LEDs (right). Reproduced with permission.[66] Copyright 2014, American Chemical Society. B, Schematic diagram illustrating omnidirectional printing (left) n silver interconnect arch printed used for LED (right). Reproduced with permission.[67] Copyright 2009, AAAS. C, Patterned illumination of 3D exposure dose to a photoresponsive material and an uncured 3D model. Reproduced with permission.[68] Copyright 2019, AAAS. D, Schematic of a printer for continuous liquid interface production, and a printed Eiffel Tower model. Reproduced with permission.[69] Copyright 2015, AAAS

formed by optical methods not only guarantees the precision, but also greatly improves the forming speed. This modified 3D printing methods is promising for large-scale industrial applications.

3 | MATERIALS

3.1 | Silicon

As the basis of modern electronics, silicon is widely used in the semiconductor industry and has desirable biocompatible and biodegradable characteristics.[76] At the same time, it has unique mechanical properties as well as electrical, optical, and biological adhesion properties.[77] While currently most applications are based on single-crystalline silicon wafers, many researchers are also focusing innovative silicon structures with various configurations. For example, Luo et al[78] created a method named atomic gold-enabled 3D lithography to produce silicon with mesostructures and they succeeded in making skeleton-like silicon (Figure 5A). Jiang et al[79] applied CVD to form a Si mesoporous structure (Figure 5B), which had amorphous atomic structure, ordered nanowire-based framework, and random submicrometer voids, with the average Young's modulus 2 to 3 orders of magnitude smaller than that of single-crystalline silicon. Kirigami-based concepts were also introduced to form strategically configured arrays of cuts to guide buckling/folding processes in a manner that reduced mechanical stresses, to form a variety of 3D structures. For example, Zhang et al[80] created a new method to fabricate complex 3D structure of the device (Figure 5C), providing a new idea for the design of silicon electronic products.

In terms of the application of silicon-based devices, the miniaturization and the precision trend are gradually presented. In the field of biological signal detection, researchers are committed to developing new detection methods with Si similar to conventional patch-clamp techniques. Tian et al[84] found that variation of reactant pressure during silicon nanowire growth could introduce reproducible 120° kinks and that the junction regions could be doped to create p-n diodes and field-effect transistors (FETs). With this method, a two-terminal FET

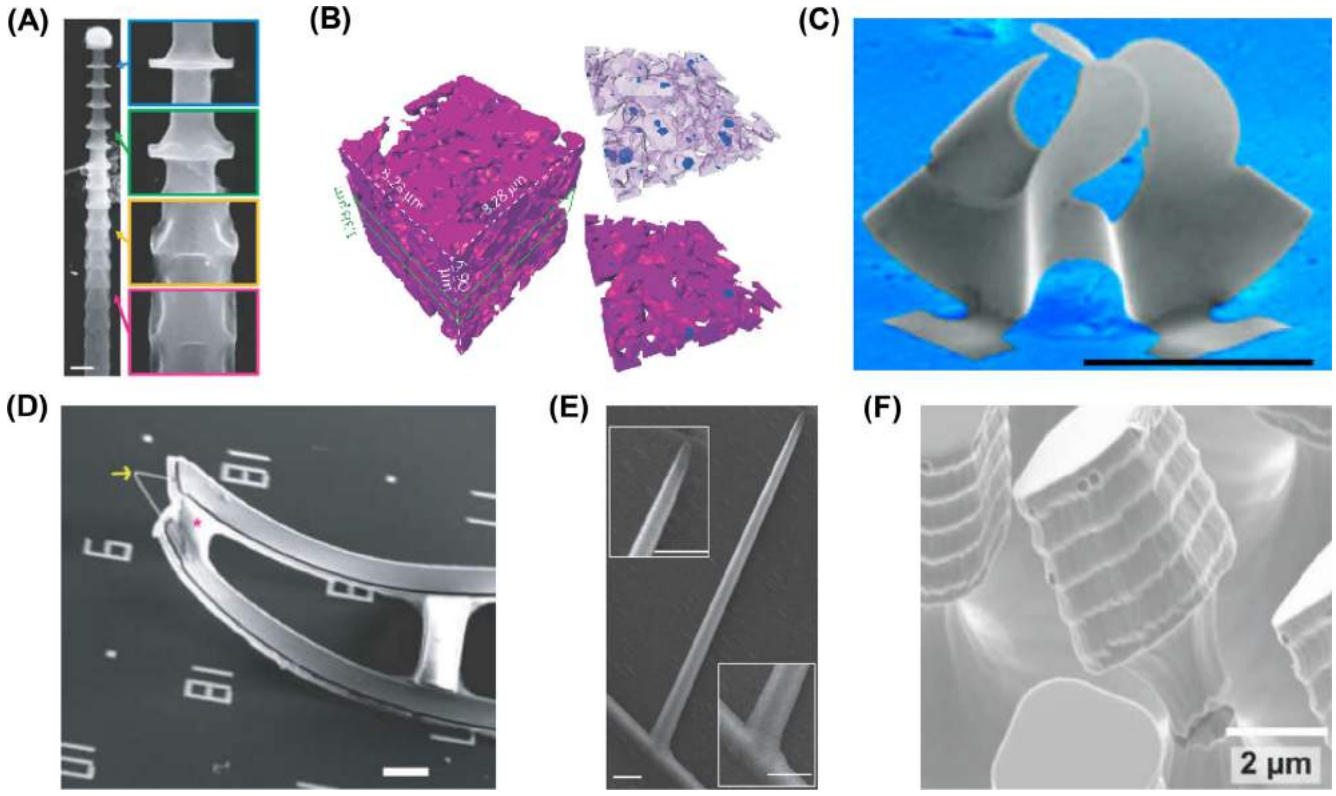

FIGURE 5 A, Scanning electron microscopy (SEM) images of skeleton-like Si spicules. Reproduced with permission.[78] Copyright 2015, AAAS. B, 3D transmission X-ray microscopic image of a mesostructured silicon scaffold. Reproduced with permission.[79] Copyright 2016, Nature Publishing Group. C, A silicon 3D structure driven by mechanical buckling. Reproduced with permission.[80] Copyright 2015, PNAS. D, SEM image of a silicon-based kinked transistor. Reproduced with permission.[81] Copyright 2010, AAAS. E, SEM image of a SiO_2 nanotube on a silicon nanowire. Reproduced with permission.[82] Copyright 2012, Nature Publishing Group. F, SEM images of bare silicon microphotodiodes. Reproduced with permission.[83] Copyright 2017, Wiley-VCH

probe (Figure 5D) was fabricated and could be inserted into single cell, to realize nanoscale neural interrogation.[81] In this design, the kink configuration and device designed places limited the probe size and the potential for multiplexing. To solve this problem, Duan et al[82] integrated SiO_2 nanotube on top of a nanoscale FET (Figure 5E). This nanotube could penetrate the cell membrane and could bring the cell cytosol into contacting with the FET, which was able to record the intracellular transmembrane potential. Silicon nanomaterials also play an important role in the field of optoelectronics. Vargas-Estevez et al[83] reported suspended silicon microphotodiodes (Figure 5F) for biological applications and the devices were able to achieve the photovoltaic detection in liquids.

To summarize, as a biocompatible and biodegradable versatile material, Si-based functional 3D structures have become useful tools in biology within recent years. There are still significant issues that need to be resolved in the future research, for example: (a) the mechanical mismatch between Si and biosystems; (b) heterogenous integration of Si with other traditional biomaterials; and (c) fundamental mechanisms of interactions between Si and biosystems (eg, how the complex bioenvironment influences the surface state of Si, which further affects its optoelectronic performance; moreover, how the cells respond to the electrical signals produced by Si-based electronics).

3.2 | Other inorganic semiconductors

Apart from elemental semiconductors like Si, C, and Ge, compound semiconductors with 3D geometries have also been exploited for biological studies because of their unique optoelectronic properties as well as ideal biocompatibility. When semiconductors are made into nanorods arrays, qualitative differences (such as localized interfaces penetrated with cells) readily take place and lead to new phenomena of 3D biointerfaces. Numerous researches have concentrated on 3D configurations for semiconductor nanorods arrays to uncover unicellular activities, multicellular connections, and growth features of biological tissues.

Presently, zinc oxide (ZnO), a biocompatible wide bandgap semiconductor as transparent intracortical microprobe was first developed as a tool to deliver light stimulus and recording biosignals simultaneously for optogenetics.[85] In the process, electrically conductive and optically transparent n-type ZnO slabs (~2 mm in thickness) were used as the raw material, and the final transparent core-shell (ZnO@ITO, indium tin oxide) probe was manufactured through a series of microfabrication steps, including micropatterning, metallic deposition, mechanical dicing, and chemical etching. Figure 6A (left) shows a scanning electron microscopy (SEM) image of a probe with smooth tips covered by an ITO conducting layer. Finally, the fabricated probe arrays (Figure 6A, right) provided a multifunctional platform for multichannel optical stimulation and recording in a rodent model in vivo.

Traditional III-V compound semiconductors, for example, indium phosphide (InP), and gallium phosphide (GaP), have been extensively investigated as functional scaffolds to regulate the growth of neuronal networks and record cellular responses from external stimuli. As demonstrated in Figure 6B,[86] the isotropic InP nanorods fabricated by microfabrication process not only monitored the neurite growth, but also promoted interactions (synchronization of calcium ion activities) among the adjacent neurons. Although the cultured cells spontaneously engulfed these III-V nanostructures, the cell adherence and survival rates on vertical III-V nanorods or nanowires are similar to those on conventional planar glass substrates, exhibiting ideal biocompatibilities (Figure 6C).[87] Using the VLS process we previously reviewed, semiconductor heterostructures with unique electronic and photonic properties can be formed and applied for biological studies. As shown in Figure 6D, the direct bandgap (tunable) GaInP segments embedded in the epitaxial GaP-GaInP axial nanowires yielded strong photoluminescence emission and acted as fluorescent indicators to visualize and identify nanowires in situ in living cells.[88] This work opened doors to track cells during the culture and proliferation processes by labeling cells in a more moderate physical manner in contrast to using chemical fluorescent reagents. Possible studies in the future would incorporate optoelectronic materials with improved biocompatibility, cytotoxicity, and even biodegradability.

3.3 | Carbon-based materials

Carbon has captured broad interests in the science community since the discovery of its diverse allotropes and derivatives, including diamonds, graphite, fullerenes (C60), carbon nanotubes (CNTs), and graphene. These various carbon-based materials present unprecedented physical and chemical properties, such as high mechanical strength, corrosion resistance, electrical, and thermal conductivities.[89] Due to these unique features, they are not only utilized in a broad range of applications including optoelectronics,[90] energy storage,[91] but also served as unique platforms for advanced bioscience exploration and biomedical engineering, such as drug delivery,[92] tissue scaffold reinforcement,[93] as well as cellular modulation and sensing.[12]

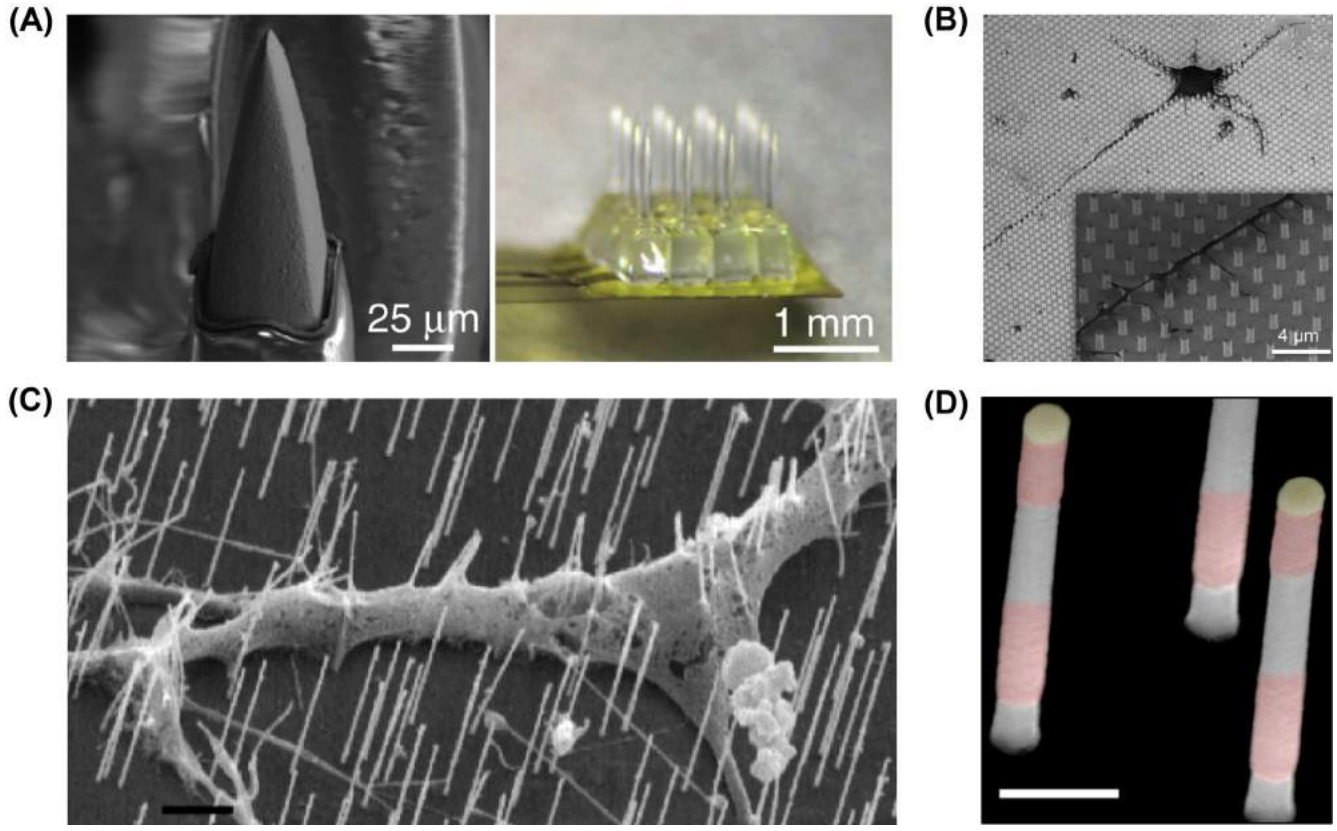

FIGURE 6 A, Scanning electron microscopy (SEM) image of a smooth ZnO tip covered by an ITO overlayer (left), and photo of a 4 × 4 optoelectrode array (right). Reproduced with permission.[85] Copyright 2015, Nature Publishing Group. B, A neuronal cell cultured on InP nanowires. Reproduced with permission.[86] Copyright 2017, American Chemical Society. C, SEM image of the cell engulfing nanowires encountered along its path, scale bars 1 μm. Reproduced with permission.[87] Copyright 2007, American Chemical Society. D, False color SEM image of GaP-GaInP dual fluorescent segment barcode nanowires (red: GaInP; gray: GaP; yellow: gold seed particle), scale bar 250 nm. Reproduced with permission.[88] Copyright 2013, American Chemical Society

CNTs have become one of the most widely used carbon-based materials since their discovery. Commonly synthesized via CVD, CNTs have a wide range of physical properties induced by extended sp^2 carbon atoms and variable geometrical parameters (eg, length, diameter, single-walled, and multiwalled). Therefore, CNTs have attracted considerable attention in biological sciences, and numerous studies have been performed on interactions between CNTs and living biosystems. For example, multiwalled CNTs (MWCNTs) were shaped into 3D architectures as scaffolds for cell seeding and growth, as shown in Figure 7A.[94] The process began with the formation of perpendicularly aligned MWCNTs by CVD on Si substrates, followed by treatments in acid solutions. This process induced capillary and tensile forces between the vertical aligned tubes, leading to 3D honeycomb-like polygons with perpendicular walls. Furthermore, these MWCNTs-based 3D scaffolds were demonstrated to support the cell attachment and growth of mouse fibroblasts by providing with bionic dimensional matrices. More recently, a vertically aligned CNT-based impedance sensor was introduced for the detection of cancer cells.[95] As shown in Figure 7B, the CNT array acted as an adhesive and electrically conductive scaffold to monitor cell behaviors with high sensitivities and spatio-temporal resolutions.

Graphene is a representative 2D material consisted of a freestanding layer with hexagonal sp^2-hybridized carbon atoms. For its unique atomic structure, graphene also possesses notable electronic characteristics like CNTs. For example, graphene shows an integer quantum Hall effect at room temperature and its band structure exhibits a Dirac fermion behavior with linear energy dispersion.[97,98] The graphene family contains members such as graphene sheets, reduced graphene oxide, graphene oxide, and layered graphenes. Recent studies have shown that single or multilayered graphene sheets and its derivatives like graphene oxides exhibit unique properties for advanced biological interfaces. Pampaloni et al[12] showed that single-layer graphene could modulate neuronal communication and excitability, by regulating extracellular ions at the

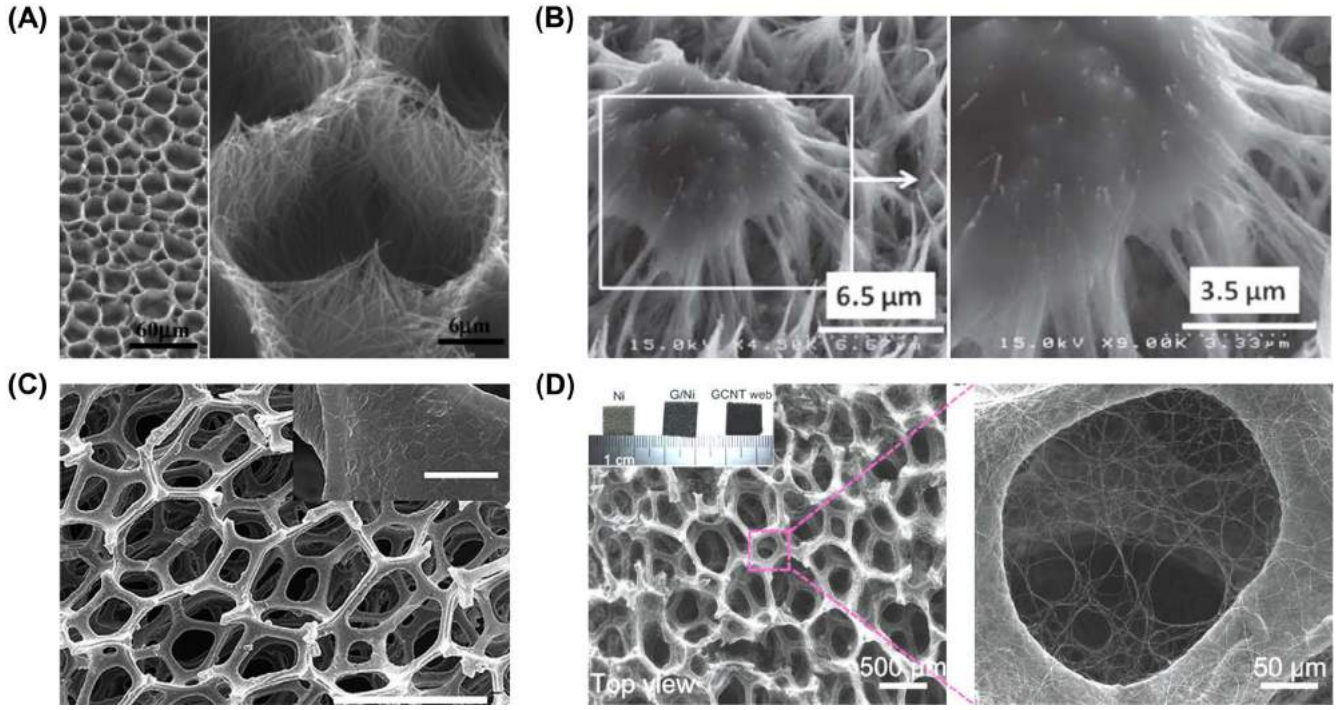

FIGURE 7 A, Scanning electron microscopy (SEM) images of a carbon nanotube (CNT) network (left) and the walls forming cavities (right). Reproduced with permission.[94] Copyright 2004, American Chemical Society. B, SEM images of an entrapped cell on CNT beams (left) and the CNT tips enter the cell (right).[95] Copyright 2012, The Royal Society of Chemistry. C, SEM image of a 3D graphene foam scaffold (scale bar 1 μm); the inset presents ripples on surface (scale bar 50 μm). Reproduced with permission.[15] Copyright 2016, Nature Publishing Group. D, Low- (left) and high-magnification (right) SEM images of the graphene-CNT web (inset: the optical images of porous nickel, graphene/nickel foam, and graphene-CNT web). Reproduced with permission.[96] Copyright 2018, Wiley-VCH

graphene/cell interface. In order to understand different dynamic behaviors of 2D and 3D biointerfaces between graphene and neuronal networks, Severino et al[15] quantitatively analyzed the growth of rat hippocampal neurons using 2D graphene films and 3D graphene foams (3D-GFs) scaffolds (Figure 7C). in vivo cell dynamics of neuronal networks cultured on the 3D-GFs showed significantly enhanced cell connectivity and more synchronous electrical activities compared to those on 2D graphene films. Furthermore, Xiao el al[96] proposed a fully interconnected graphene-CNT hybrid 3D web to study glioma infiltration in engineered 3D cortex-like networks, as shown in Figure 7D. Such a 3D cortex-like network responded to dense neuronal networks and exhibited functional activities close to cells at in vivo conditions. Although their biocompatibility and cytotoxicity need further investigation for in vivo and clinical applications in the future,[99] these carbon-based functional 3D networks provide promising solutions for bioactive interfaces.

3.4 | Metallic meshes

In the past years, electrically conductive mesh electronics (mostly metal based) have received tremendous attentions for the study of biointerfaces. With careful designs, these thin-film, mesh-based metallic structures realize similar mechanical properties (eg, bending stiffness) to biological tissues.[100] Additionally, they electronically record and/or regulate biological signals in biological environments, with high spatial-temporal resolutions.[101] Here, we highlight some latest studies on metallic mesh electronics and their relevance to specific biomedical applications.

Figure 8A shows ultraflexible multichannel mesh electronics with a low Young's modulus that were injected into mouse eyes.[102] Compared with semiconductor and ceramic based materials, these metallic meshes were able to form compact and more conformal coating on the retina surface, obtaining reliable recording of individual retinal ganglion cells in vivo. Figure 8B further illustrates a "neurotassel" structure consisting of 1024 microelectrodes, which was developed via microfabricarion process coupled with elastocapillary self-assembly when withdrawn from molten poly(ethylene glycol) (PEG).[103] Such a neurotassel was demonstrated to collect electrical signals from a large number of neurons in the deep brain of rodents. Figure 8C illustrates an active hybrid cardiac patch system with multifunctional mesh electrodes to monitor and regulate cardiac

functions ex vivo.[104] Other than general mesh electronics only for biosignal recording, this patch system was empowered to precisely release biochemical factors for function enhancement of cardiac tissues.

3.5 | Conductive polymers

Conventional electrodes made of metals like gold, titanium, and platinum or semiconductors like silicon usually have smooth surface and high electrical impedance with interfacing with biological tissues. Therefore, it is crucial to apply materials that match with biotissues in various aspects, to enhance the signal quality.[105,106] Soft conductive polymers can reduce the mechanical mismatch, the impedance at tissue interfaces, and the inflammatory response.[107,108] For example, polypyrrole (PPy), as a traditional conductive polymer with ideal biocompatibility, has been developed and applied for biosensors in various areas. Qi et al[109] fabricated a microelectrode array (MEA) made of modified PPy nanowires (Figure 9A). These PPy nanowires enhanced adhesion between the MEA and the neural tissue (Figure 9B), and resulted in higher softness and lower impedance (at lower frequencies, below 100 Hz) than those made of the gold electrodes.

Long-distance peripheral nerve defects are one of the major challenges in clinical medicine. A series of recent studies[112,113] have shown that electrical signals play an important role in promoting and guiding peripheral nerve growth. In the area of nerve repair, conductive polymers can be used to establish electrically active scaffolds for tissue engineering. As shown in Figure 9C,D, Huang et al[110] combined PPy with chitosan and fabricated a conductive scaffold with microchannels for nerve repairing, which could generate an electric field at the site of nerve injury and thus promote nerve growth. With a similar approach, Xu et al[111] integrated PPy with poly (D,L-lactic acid) (PDLLA) to create a conductive nerve repair scaffold (Figure 9E). The combination of the excellent mechanical property and biodegradable property of PDLLA with the electrical conductivity of PPy showed a great potential in repairing long-distance peripheral nerve defects. Future research directions include the

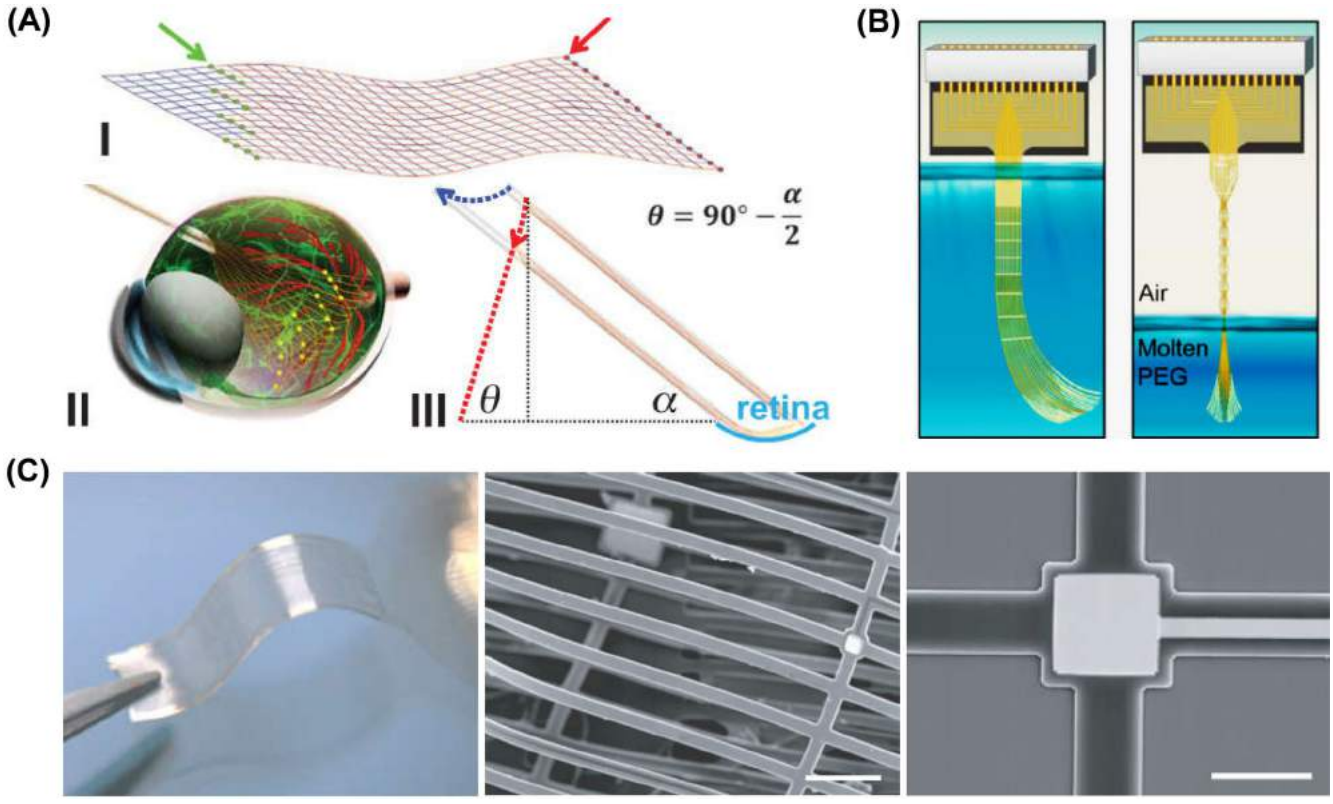

FIGURE 8 A, Schematics showing the noncoaxial intravitreal injection of mesh electronics onto the RGC layer. Reproduced with permission.[102] Copyright 2018, AAAS. B, Schematics of the elastocapillary self-assembly of a neurotassel. Reproduced with permission.[103] Copyright 2019, AAAS. C, Image of a freestanding flexible device consisting of 32 gold electrodes (left), scanning electron microscope images of a rolled device as presented in the dashed square (middle, scale bar 200 μm) and a 50 × 50 μm^2 electrode pad (right, scale bar 50 μm). Reproduced with permission.[104] Copyright 2016, Nature Publishing Group

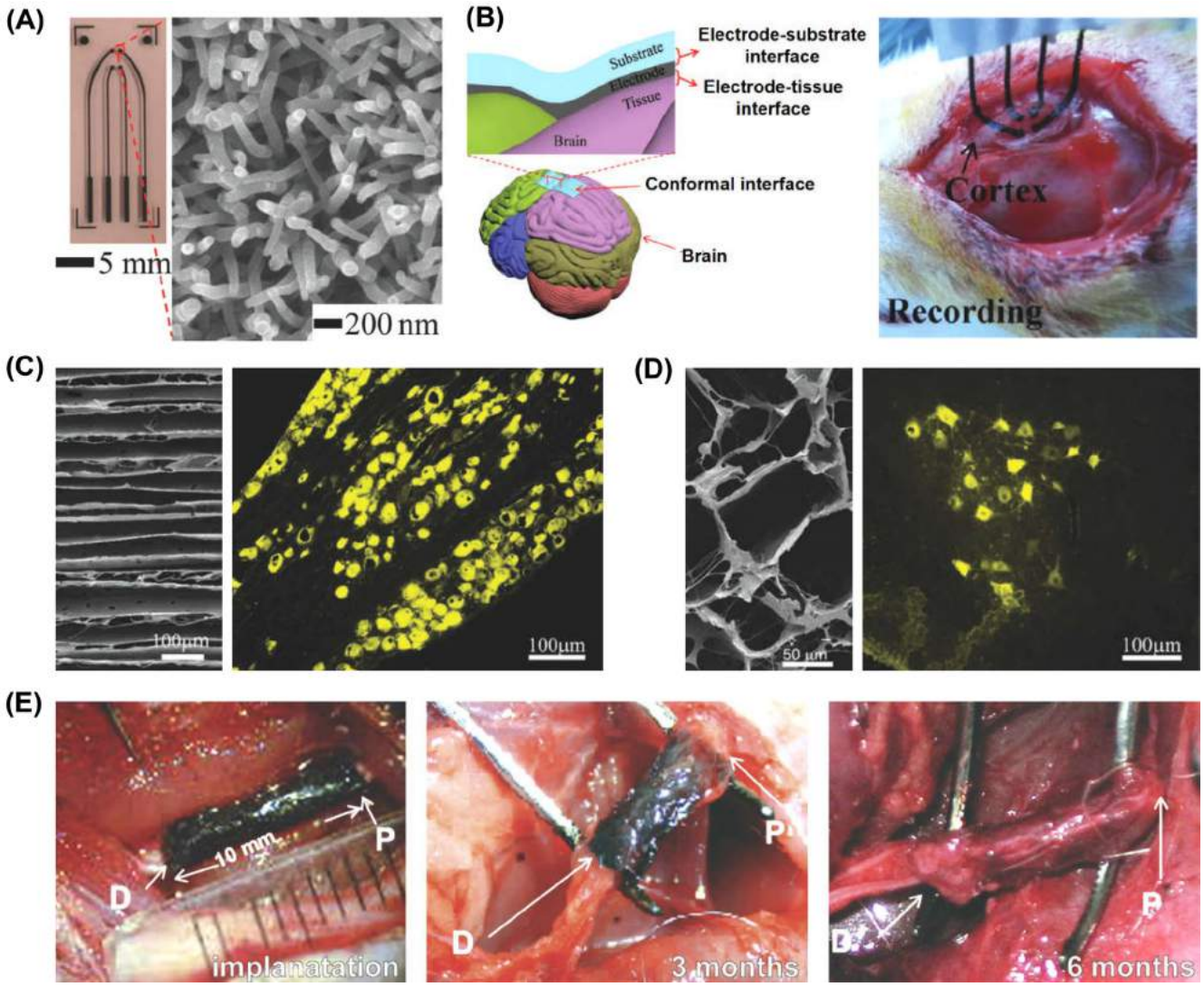

FIGURE 9 A, Optical image of the multielectrode array on an ITO glass substrate (left) and scanning electron microscope image of the PPy nanowires (right). B, Schematic of the compliant electrode array adhering to a rat brain (left) and image of a four-channel MEA on the brain. Reproduced with permission.[109] Copyright 2017, Wiley-VCH. C, D, Microstructures of a conductive chitosan/polypyrrole scaffold and images of FG-positive motoneurons in the scaffold. Reproduced with permission.[110] Copyright 2012, PLOS. E, Intraoperative photographs of the PPy/PDLLA nerve conduits, immediately after grafting (left), 3 months postoperatively (middle), 6 months postoperatively (right). Reproduced with permission.[111] Copyright 2013, Elsevier

improvements in materials' stability and degradability for in vivo applications.

3.6 | Hybrid scaffolds

Due to the mechanical properties and topographic structures of traditional 2D electronic devices, their applications are severely limited in fields like tissue engineering and 3D architectures are necessary. Furthermore, hybrid 3D structures can take the advantages of different materials and exhibit unique functionalities. For example, after a heart attack, 3D porous materials are often used as a heart patch to grow heart cells to repair damaged tissue.[114,115] Dvir et al[116] developed a 3D scaffold made of alginate and gold nanowires. By using gold nanowires to bridge nonconductive pore walls of alginate scaffolds (Figure 10A), these composite 3D scaffolds could improve electrical communication between cardiac cells. Currently, in tissues regeneration, most techniques of optical imaging[119] and planar microelectrodes[120,121] are limited to a 2D plane. Tian et al[117] integrated polymer scaffolds with FETs made from silicon nanowires through lithography, obtaining a 3D macroporous nanoelectronic scaffold (Figure 10B). By using silicon nanowire FETs, the 3D scaffold was able to record both extracellular and

intracellular signals from cultured neural cells.[122] Via a similar method, Dai et al[118] fabricated tissue-scaffold-mimicking 3D nanoelectronic arrays (Figure 10C), which realized real-time monitoring of extracellular action potentials in cardiac tissues. In these hybrid 3D scaffolds, various devices can be integrated, such as chemical sensors,[123] pressure sensors,[124] and light-emitting devices.[125]

4 | APPLICATIONS

4.1 | Cell culture

In vitro cell culture technologies have revolutionized our understanding of cellular behaviors. Owing to the complex 3D topography, the ECM holds sophisticated biochemical and mechanical properties, which precisely controls cellular organization and modulates the tissue growth. Therefore, the construction of bionic 3D templates as desirable extracellular microenvironments is imminently required for cell culture. Using organic-based biocompatible and biodegradable materials to construct 3D scaffolds have been broadly exploited.[21] Conventional biodegradable materials are usually based on natural-derived materials such as collagen, silk, hydrogels, and synthetic polymers such as poly(lactic acid), poly(glycolic acid), and their copolymer poly(lactic-co-glycolide) (PLGA).[126] As a representative example shown in Figure 11A, a poly(2-hydroxyethylmethacrylate)-based hydrogel was printed to form periodic 3D scaffolds, creating 3D environments for neuronal cell culture.[127] Confocal images of representative neuronal cells on the scaffolds revealed that cells preferred wrapping around junctions of the orthogonal intersections between printed rods in adjacent layers. As an electrically conductive, optically transparent and biocompatible material, PEDOT:PSS was also used to fabricate macroporous scaffold via ice-templating method for fibroblast culture.[128] The SEM image in the top of Figure 11B indicates the stromal cells successfully invaded and adhered to the PEDOT:PSS scaffold. The fluorescence image (Figure 11B, bottom) further demonstrates that the cells were capable to polymerize fibronectin into fibers, indicating that the cells were performing regular cell functions in this PEDOT:PSS-based ECM.

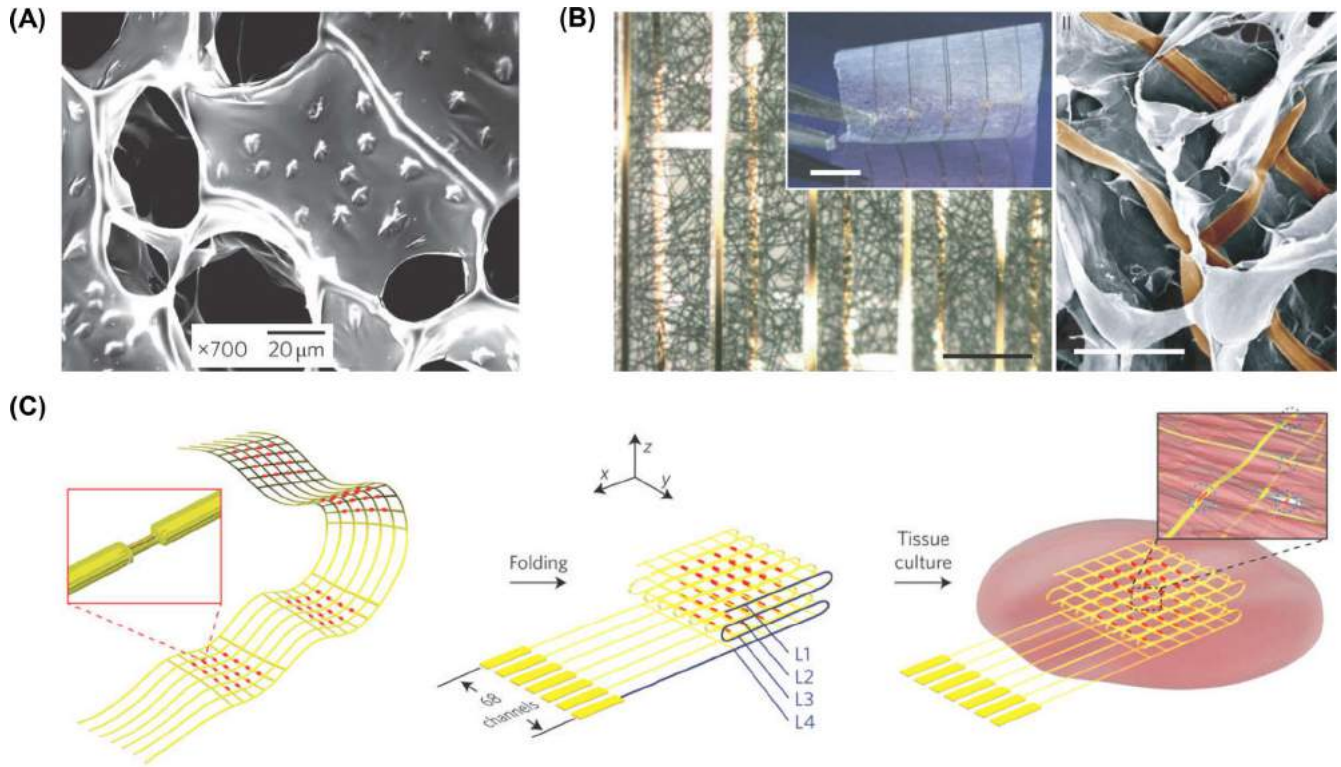

FIGURE 10 A, Scanning electron microscopy (SEM) image of nanowires assembled within the pore walls of the scaffold into star-shaped structures. Reproduced with permission.[116] Copyright 2011, Nature Publishing Group. B, A bright-field optical micrograph of the folded scaffold, the inset showing a hybrid sheet before folding (scale bars, left: 200 μm and inset: 5 mm), SEM image of a mesh nano-ES/alginate scaffold (right, scale bar 100 μm). Reproduced with permission.[117] Copyright 2012, Nature Publishing Group. C, Schematic of the freestanding macroporous nanoelectronic scaffold with nanowire FET arrays (red dots). Reproduced with permission.[118] Copyright 2016, Nature Publishing Group

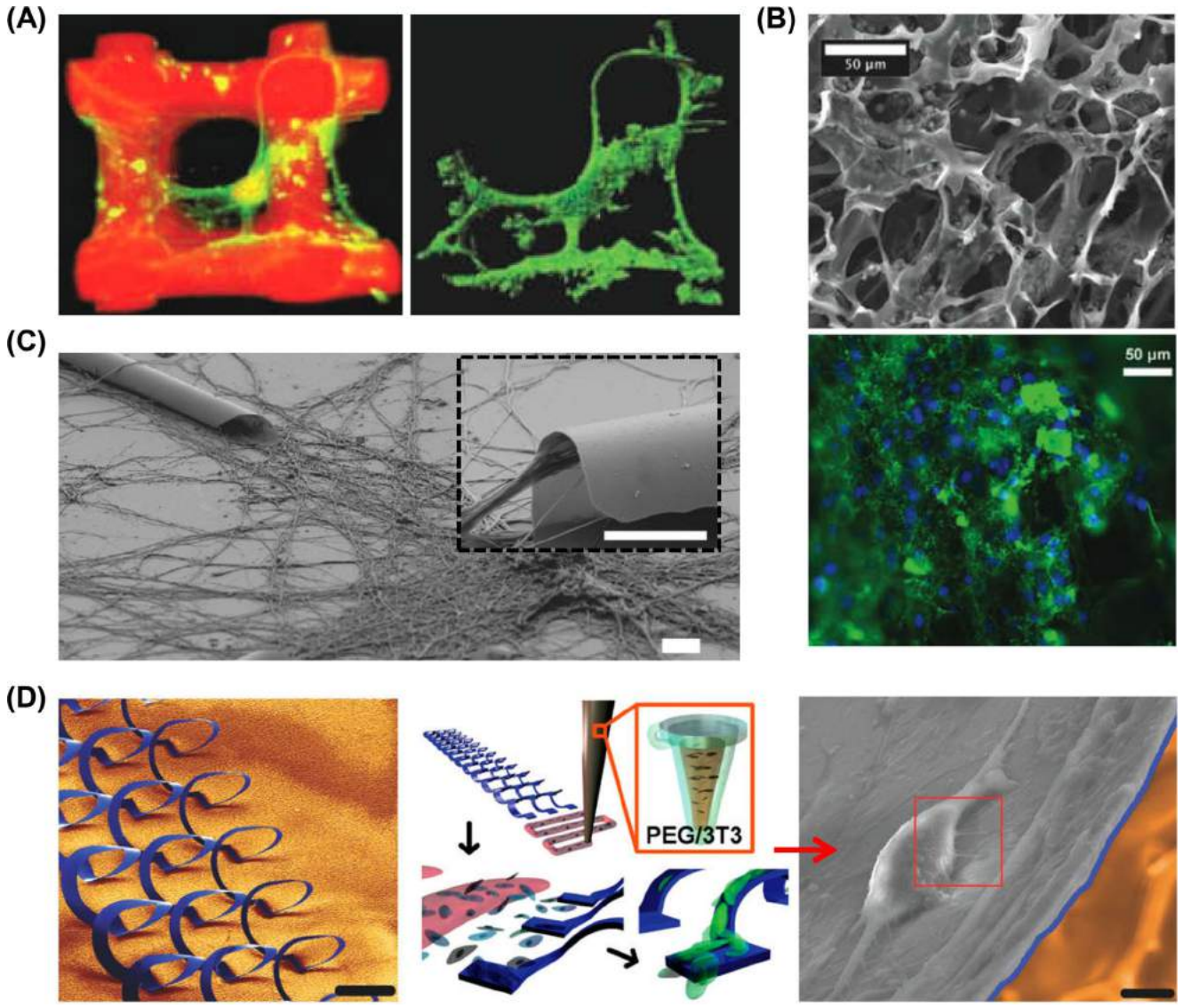

FIGURE 11 A, Confocal images of neuronal cells on the scaffolds (left) and soma on scaffold (right, scale bar 20 μm). Reproduced with permission.[127] Copyright 2011, Wiley-VCH. B, Scanning electron microscopy (SEM) image of a PEDOT:PSS scaffold after cell culture (top), and its fluorescence micrograph with cell-deposited fibronectin fibers (bottom). Reproduced with permission.[128] Copyright 2015, Royal Society of Chemistry. C, SEM image of Si/SiGe nanotubes for controlled neurite outgrowth (scale bar 10 μm, and 5 μm for inset). Reproduced with permission.[129] Copyright 2011, American Chemical Society. D, Colorized SEM image of a solenoid array (left, scale bar 500 μm), schematics of DIW poly(ethylene glycol)/media-3T3 gel deposited locally onto the solenoid array (middle), and a migrating 3T3 cell on the solenoid array (right, scale bars 5 μm). Reproduced with permission.[130] Copyright 2017, Wiley-VCH

The exploration of interfaces between biological systems and semiconductors has also attracted considerable attentions. Illustrated in Figure 11C, Si and Ge nanomembranes were transformed to nanotubes by strain induced self-rolling, which were employed as 3D culture platforms for primary cortical neurons.[129] When interacting with surfaces of these 3D nanotubes, neural cells maintained their normal morphology when interacting with Si or SiGe surfaces, and they presented a growth preference within and along the 3D nanotubes.

In Figure 11D, McCracken et al[130] conducted a comprehensive study by using a Si-based microscale 3D framework to regulate cultured cell behaviors. The Si-based 3D scaffolds were fabricated via the compressive force-guided assembly mentioned in previous sections (Figure 11D, left). A 3T3 (3-day transfer, inoculum 3×10^5 cells) fibroblasts/media/PEG gel suspension was applied as the printing ink and directly written onto the Si scaffolds. After the dissolution of PEG gel suspension, the 3T3 cells adhered to the Si scaffolds and migrated along the ribbon framework (Figure 11D, middle).

Figure 11D (right) shows the 3T3 cell's morphology as it migrated along the Si ribbons, and the highlighted red region demonstrates that the filopodia could anchor the cells to the scaffold. Furthermore, these Si-based 3D scaffolds were also well adapted to the morphology of dorsal root ganglion neurons at the tissue-level organization.

4.2 | Recording and sensing

Monitoring in vitro and in vivo biological activities is essential to understand animal behaviors and provide instructive insights to clinical diagnostics. For example, recently explored advanced epidermal sensors respond to

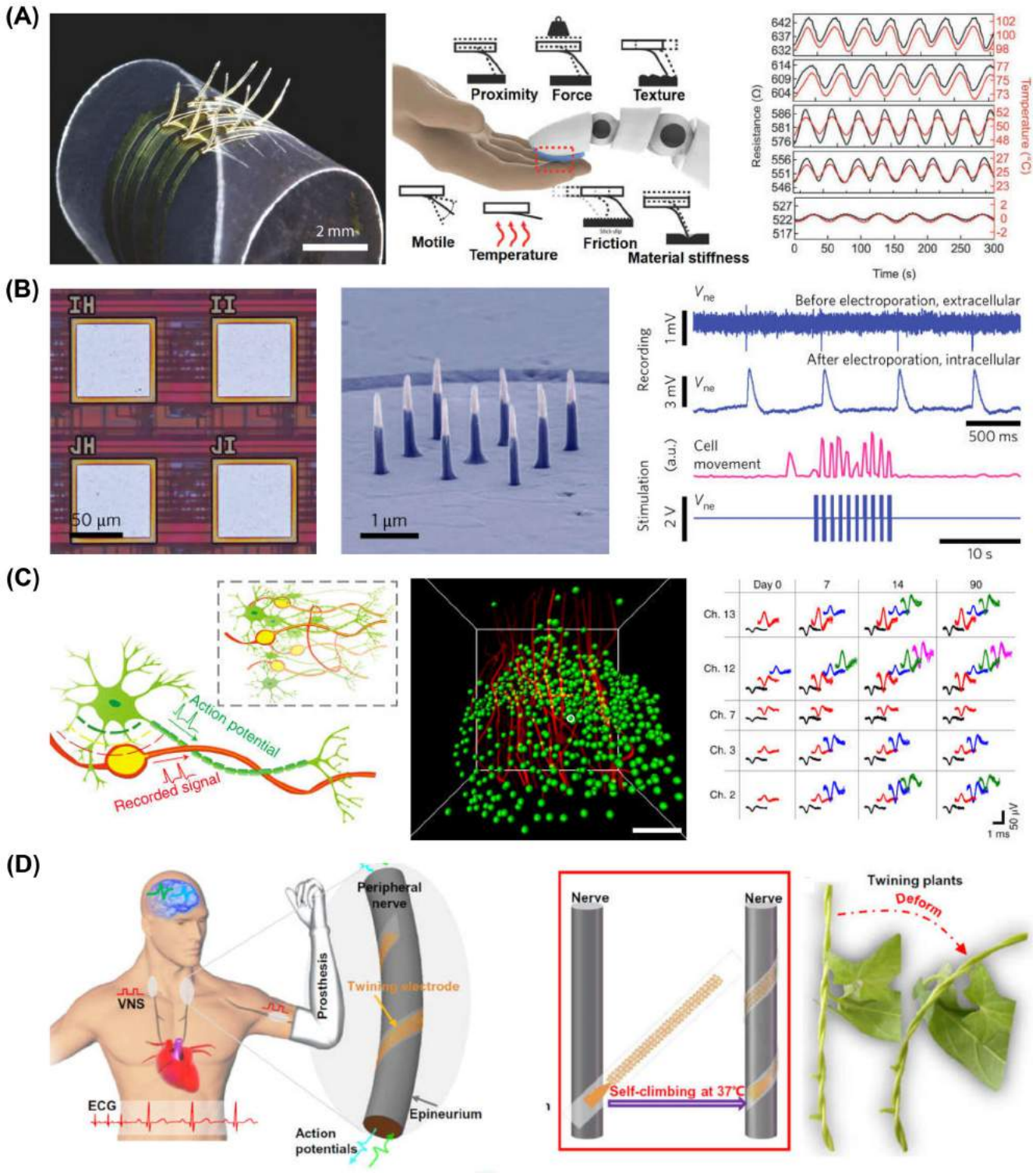

FIGURE 12 Legend on next page.

various stimuli on the human skin, like pressure, temperature, surface roughness, and material hardness, with potential applications in the development of artificial limbs, robot sensors, and wearable electronic devices.[131-133] Sensor platforms based on assembled electronic and optical devices on soft substrates have been intensively investigated, such as all-graphene multifunctional electronic skin sensor matrices,[134] fully printed fingerprint-like three-axis tactile force and temperature sensors,[135] and user-interactive electronic skins.[124] Specifically, innovations on the 3D structural design for these active sensors are of particular interest. Shown in the left of Figure 12A, Reeder et al[136] fabricated a device matrix with novel sensing modalities, named electronic whiskers (e-whiskers). The e-whisker imitated the characteristics of animal whiskers by using a gold strain gauge on a flexible substrate made of a shape memory polymer. In such a shape memory-based reconfigurable structure, the strain gauge was empowered to probe various stimuli such as proximity, surface topology, friction, force, material stiffness, and temperature (Figure 12A, middle and right). Another example is the microelectrode system for the electrophysiological recording of living cells, along with sensors for optical imaging based on luminophores like Ca^{2+} indicators,[140] potentiometric dyes,[141] and voltage-sensitive proteins.[142] While the conventional patch-clamp technique has been widely applied for high-precision extracellular and intracellular recordings, recently developed complementary metal-oxide-semiconductor (CMOS) microelectrode arrays (MEAs) are able to collect signals for a large group of cells.[143-145] Abbott et al[137] fabricated arrays of nanoscale probes coupled to a fully integrated circuit based on the 0.35-μm CMOS technology (Figure 12B, left and middle), which captured intracellular potentials for individual neurons in a large-scale cellular network (Figure 12B, right).

In regard to implantable electrodes for in vivo neural recording, Michigan-type microelectrode arrays[146] and Utah arrays[147] are widely used; however, these Si-based, rigid probes induce tissue inflammation and lead to undesirable biocompatibility. Further technology developments require optimized soft nerve electrodes that possess mechanical properties conformable to those of brain tissues.[129] Inspired by the morphology of the neuron network, Yang et al[138] developed lithographically defined metal electrodes on polymer substrates to produce neuron-like electronics (NeuE) at the subcellular level (Figure 12C). The geometry of NeuE matched to that of neuron cells, with similar mechanical properties such as stiffness. Inspired by the natural spiral structure of twining plants,[148] Zhang et al[139] fabricated twining electrodes (Figure 12D) by using shape memory polymers. With significantly reduced mechanical mismatches and sliding frictions between electrodes and surrounding tissues, these deformable electrodes could swag, bend, and stretch with the peripheral nerve at the body temperature (~37°C) without additional surgical fixation.

4.3 | Regulation and modulation

Besides biological sensing, advanced 3D biointerfaces also play critical roles in the stimulation and function regulation of brains, spinal cords, peripheral nerves, cardiac, and other organ systems.[149-151] For neural modulation we focus here, conventional techniques based on electrophysiology and optogenetics have been widely applied. For these methods, electrical and/or optical signals are applied to activate or inhibit specific ion channels, thereby adjusting neuron activities. Implantable devices for electrical neuromodulation have been widely used in clinical practice, such as deep brain stimulators and vagus nerve stimulators.[152] To reduce the mechanical mismatch, soft materials like hydrogels are used as the interface between devices and tissues.[153] However, the low conductivity of conventional hydrogels makes them unable to respond quickly to high-frequency signals, and they are difficult to be patterned using standard micro- and nanoprocessing technologies. To overcome these challenges, Liu et al[154] developed a highly electrically conductive hydrogel and devised a process to lithographically pattern it, forming a hydrogel based electrode array (Figure 13A). These electrodes exhibited a high-charge

FIGURE 12 A, A bended array of electronic whisker (left), its sensing modalities using 3D electronic whiskers (middle), and resistance response to temperature fluctuations (right). Reproduced with permission.[136] Copyright 2018, Wiley-VCH. B, Four pixels in the 32 × 32 array (left), false-colored scanning electron microscope image of nine vertical nanoelectrodes fabricated per pad (middle, the tip with white color was Pt, and the base with blue color is SiO_2), extracellular and intracellular recordings of cardiac action potentials (right). Reproduced with permission.[137] Copyright 2017, Nature Publishing Group. C, Schematics showing the neuron-like recording network (left), 3D image of NeuE near the CA1 subfield (middle, scale bar 50 μm), time evolution of spikes of principal component analysis clustered single units from five representative channels (right). Reproduced with permission.[138] Copyright 2019, Nature Publishing Group. D, Schematic diagram of the conceptual PNS neuromodulation for restoring the motor and physiological functions and the electrode-nerve interface (left), the self-climbing process from the flattened state driven by body temperature and the photograph of the twining plants during deformation (right). Reproduced with permission.[139] Copyright 2019, AAAS

storage capability and long-term stability in the physiological environment. They were placed on the sciatic nerve of mice and showed desirable performance for chronic stimulation.

In the early 2000s, the discovery of light-sensitive ion channels and their transformation into neurons led to the rise of optogenetics.[157] Due to the strong absorption and scattering of biological tissues, implantable light sources are required for light delivery into the deep brain. Kim et al[155] fabricated injectable, cellular-scale optoelectronic devices, including microscale inorganic light-emitting diodes (μ-ILEDs), microelectrodes, and microscale inorganic photodetectors (μ-IPDs) stacked on a flexible injectable microneedle substrate (Figure 13B). Compared to conventional silica fibers, thin-film microscale optoelectronic devices printed on flexible probes can provide wirelessly operated, multifunctional neural modulation, and sensing, realizing promising solutions for ideal optical biointerfaces.

The dimensional accuracy of electrophysiological modulation is determined by the geometry of the interface between the implanted electrode and the tissue. Based on this principle, Jiang et al[156] reported an optically controlled multiscale biointerfaces by regulating the

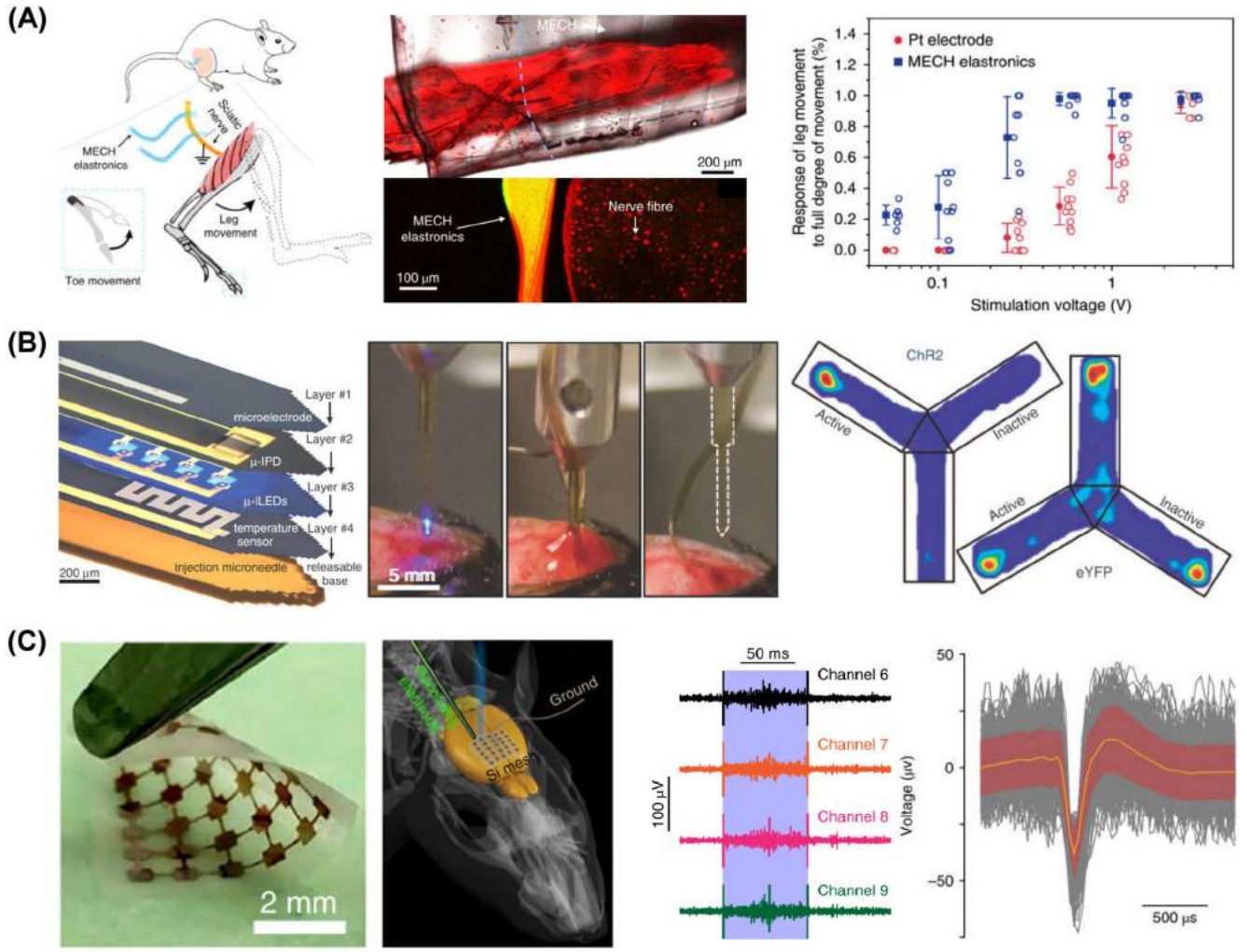

FIGURE 13 A, Schematic of the in vivo neural stimulation with a micropatterned electrically conductive hydrogels (MECH) microelectrode (left), projection of a three-dimensional reconstructed confocal micrograph of the MECH microelectrodes wrapping around a sciatic nerve (middle), the percentage of leg movement under different stimulation voltages for the MECH electrode and the platinum electrode (right). Reproduced with permission.[154] Copyright 2019, Nature Publishing Group. B, A multifunctional, implantable optoelectronic device with illustration of various components (left), process of injection and release of the microneedle (middle), heat maps of activity during the posttest (right). Reproduced with permission.[155] Copyright 2013, AAAS. C, A flexible device composed of a stack of a distributed Si mesh and a holey PDMS membrane (left), schematic illustrating the in vivo photostimulation test (middle), example traces of raw neural response and mean neuron-firing waveform (orange) superposed on individual waveforms (black) of both spontaneous and stimulation-evoked activities (right two). Reproduced with permission.[156] Copyright 2018, Nature Publishing Group

size of silicon (from nanometers to centimeters). At the nanosize scale, they created a multilayered p-i-n Si diode junction by CVD to form the intrinsic and n-type Si layers onto a p-type Si semiconductor-on-insulator substrate. At the centimeter scale, they designed a bilayer device layout, consisting of the Au-decorated Si mesh and the holey PDMS membrane (Figure 13C). Using a laser-induced photoelectric effect, the Si-based heterostructures can modulate neuron activities at both the cellular and the tissue level.

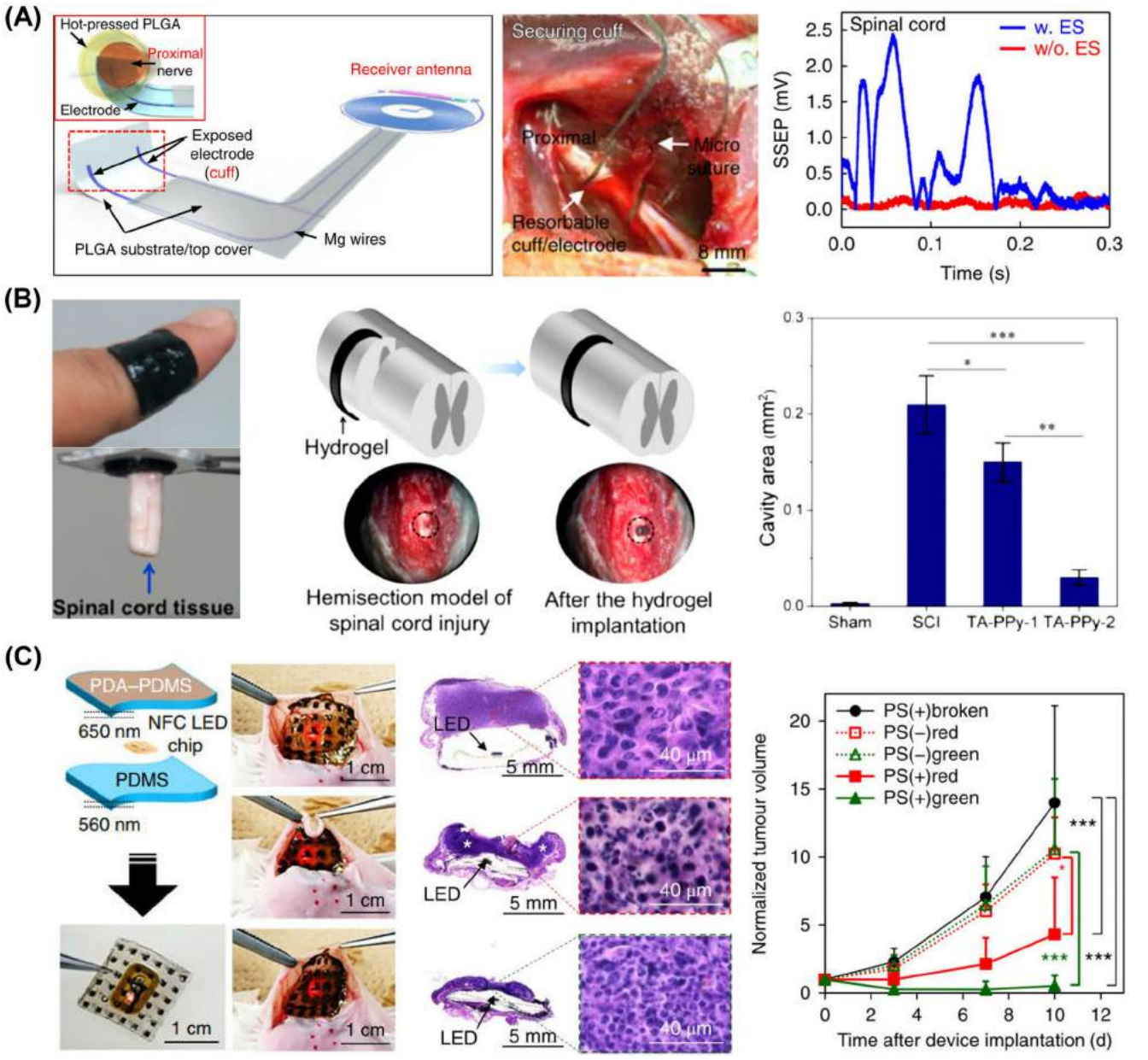

FIGURE 14 A, Illustration of a bioresorbable, wireless electrical stimulator as an electronic neuroregenerative medical device (left), its surgical procedure for implanting the device to the sciatic nerve (middle), and application in spinal cord stimulation (right). Reproduced with permission.[29] Copyright 2018, Nature Publishing Group. B, Photograph of freestanding conducting polymer hydrogel (CPH) films on a finger (left top) and demonstration of the adhesion of the CPH to spinal cord tissue in vitro (left bottom), graphical representation of semitubular CPH implanted as a bridge to cover the spinal cord hemisection gap (middle), quantification graphs showing the average cystic cavity area of animals with SCI and other treatments (right). Reproduced with permission.[159] Copyright 2018, American Chemical Society. C, Images of a sandwiched near-field communication (NFC) LED chip subcutaneously implanted on the inner surface of the dorsal skin when the skin stretched, compressed and twisted (left two), histopathological images of the intradermally transplanted tumor of the mice treated with different devices (middle), normalized tumor volume of the three control and two PDT groups of mice (right). Reproduced with permission.[160] Copyright 2019, Nature Publishing Group

4.4 | Therapy

Different from conventional pharmacological therapies that engage biochemical interplay, advanced 3D functional structures enable physical interactions (electrical, optical, and/or mechanical) with biological systems, realizing novel therapeutic functions in areas like tissue regeneration and phototherapy. For example, the effects of electrical stimulation on tissue regeneration have been investigated for decades.[158] Unlike conventional methods based on external electronic wires and instruments, Koo et al[29] developed an innovative nonpharmacological treatment to repair peripheral nerves by electrical stimulation, based on a wirelessly operated, fully implantable and bioresorbable device system. The developed platform used a radio frequency power harvester to dramatically facilitate nerve regeneration via electrical stimulation. As shown in Figure 14A (left), the device systems was comprised of fully biocompatible and degradable materials, including Si (for diode), Mg (magnesium, for coils and electrodes), and PLGA (for dielectric interlayers and substrates). The middle part of Figure 14A displays the surgical process, showing the cuff secured to the sciatic nerve with biodegradable sutures. Somatosensory evoked potential was acquired from stimulation of the spinal cord with monophasic pulses (Figure 14A, right). The in vivo results revealed that the electrical stimulation provided by such an electronic medicine could effectively promote the nerve recovery.

In another work, Zhou and coworkers developed conducting polymer hydrogels (CPHs) as a bioactive scaffold to repair spinal cord injury by bridging spinal cord lesions (Figure 14B).[159] The CPHs were engineered to achieve high electrical conductivity and appropriate mechanical properties that matched to the surrounding tissue (Figure 14B, left). Figure 14B (middle) presents the semitubular CPH covering the spinal cord hemisection gap. With the implanted CPHs, the endogenous electric microenvironment could contribute to the restoration and regeneration of interrupted nerves. Compared to the control groups, the injured animals with the electroactive gels presented accelerated nerve tissue regeneration and showed smaller cavity sizes (Figure 14B, right).

PDT is an effective method for cancer treatments based on optically activated photosensitizers.[31] Conventional PDT is limited for curing tumors on the skin surface. For applications in the deep tissue, biodegradable light sources and their seamless fixation with complex 3D biological tissues are necessary. Here, an implantable device system was demonstrated PDT in the deep tissue, by using polydopamine (PDA) as a biocompatible adhesive material for chronic fixation.[160] Figure 14C (left) illustrates the layered device structure, consisting of a near-field communication controlled LED chip and PDA-PDMS-based nanosheets. The PDA-based adhesive ensured that the subcutaneously implanted device was stably fixed onto the inner surface of the dorsal skin even under the conditions of mechanical stretching, compressing and twisting (Figure 14C, middle). By remotely operating the implanted microscale LEDs, low-dose and long-term PDT was demonstrated to successfully kill microtumors in vivo in a mouse model (Figure 14C, right). Because of the low invasiveness of suture-free implantation, this technique is expected to be an effective treatment for deep-tissue tumors in fragile and delicate organs like the brain and pancreas.

5 | CONCLUSION AND OUTLOOK

In this paper, we have reviewed recent advances of 3D electronic and photonic biointerfaces as emerging platforms for fundamental biological studies and advanced biomedical applications. While the biology systems of interest are always soft, flexible, curved, and wrinkled in complex 3D geometries, artificial high-quality materials and devices are conventionally rigid, flat, smooth, and steady.[161] The developments of novel 3D concepts and manufacturing techniques are imminently motivated to overcome this fundamental mismatch, and corresponding materials with designer structures are highly demanded. Recent progress has constructed various available techniques with encouraging abilities in forming 3D structures, as demonstrated in this article, including vapor growth, microfabrication, mechanical assembly, and so on. Challenges still remain in the aspect of accessible materials. For example, although 3D printing technologies offer outstanding capability in forming complex 3D architectures, further promotions are still needed for rapid large-scale processing and incorporating functional materials such as semiconductors as raw materials for printing. Furthermore, the design principle and standards for 3D manufacturing remains uncertain. In other words, there still exist enormous opportunities in the exploration of fundamentally effective and all-purpose strategies for forming 3D nano-, micro-, and mesostructures.

Biosystems naturally respond to and communicate via a series of physical events, such as electrical, optical, mechanical, and thermal signals. Conventional materials such as ceramics (eg, hydroxyapatite) and synthetic polymers (eg, polylactides, polycaprolactone) are able to offer proper mechanical properties and provide topographically effective bioscaffolds, but they lack bioactive properties when interacted with biosystems, which limits their biomedical applications particularly serving as scaffolds in tissue engineering. Alternatively, semiconductors display incomparable superiority because of their tunable

optical and electrical properties together with abundant signal transduction mechanisms at the biointerface, but they are inelastic or too fragile to fit with biological tissues. In addition, typical semiconductors made of bulk crystals or organics are not biodegradable and bioabsorbable, producing biocompatibility issues during chronic implantation. By modifying these active materials in a thin-film, micro-/nanoscale platform, they can be incorporated into biologically relevant structures and potentially facilitate progress toward clinically practical biointerfaces.

In spite of the preliminary results discussed here, comprehensive understanding of inner mechanisms (eg, how different cells and organelles sense the external electrical field and photons) for biological behaviors at the biotic-abiotic interfaces is necessary to provide guidance for further progress. From the aspect of the latest progress on versatile applications of such active 3D structures encompassing cell culturing, biosignal sensing/modulation, and tissue regeneration, the unique capabilities of electronic and photonic biointerfaces hold great potential for developing progressive biological technologies to realize fundamental biological studies in vitro and/or in vivo, and to advance biomedical applications in clinical practice.

ACKNOWLEDGMENTS

H. Wang and P. Sun contributed equally to this work. This work is supported by National Natural Science Foundation of China (NSFC) (61874064, to X.S.; 51601103, to L.Y.), Beijing Innovation Center for Future Chips, Beijing National Research Center for Information Science and Technology at Tsinghua University (BNR2019ZS01005), and Key Laboratory of Advanced Materials of Ministry of Education of China (XJCL201903).

CONFLICT OF INTEREST

The authors declare no conflict of interest.

ORCID

Xing Sheng https://orcid.org/0000-0002-8744-1700

REFERENCES

1. McDonough IM, Allen RS. Biological markers of aging and mental health: a seed and soil model of neurocognitive disorders. *Aging Ment Health*. 2019;23:793-799.
2. Sligo J, Gauld R, Roberts V, Villa L. A literature review for large-scale health information system project planning, implementation and evaluation. *Int J Med Inform*. 2017;97:86-97.
3. Sun TL, Qing GY, Su BL, Jiang L. Functional biointerface materials inspired from nature. *Chem Soc Rev*. 2011;40:2909-2921.
4. Nel AE, Madler L, Velegol D, et al. Understanding biophysicochemical interactions at the nano-bio interface. *Nat Mater*. 2009;8:543-557.
5. Larson DR, Zipfel WR, Williams RM, et al. Water-soluble quantum dots for multiphoton fluorescence imaging in vivo. *Science*. 2003;300:1434-1436.
6. Bruchez M, Moronne M, Gin P, Weiss S, Alivisatos AP. Semiconductor nanocrystals as fluorescent biological labels. *Science*. 1998;281:2013-2016.
7. Jamieson T, Bakhshi R, Petrova D, Pocock R, Imani M, Seifalian AM. Biological applications of quantum dots. *Biomaterials*. 2007;28:4717-4732.
8. Duan X, Fu T-M, Liu J, Lieber CM. Nanoelectronics-biology frontier: from nanoscopic probes for action potential recording in live cells to three-dimensional cyborg tissues. *Nano Today*. 2013;8:351-373.
9. Hong G, Diao S, Chang J, et al. Through-skull fluorescence imaging of the brain in a new near-infrared window. *Nat Photonics*. 2014;8:723-730.
10. Zhang A, Lieber CM. Nano-bioelectronics. *Chem Rev*. 2016;116:215-257.
11. Choi C, Choi MK, Liu SY, et al. Human eye-inspired soft optoelectronic device using high-density MoS2-graphene curved image sensor array. *Nat Commun*. 2017;8:1664.
12. Pampaloni NP, Lottner M, Giugliano M, et al. Single-layer graphene modulates neuronal communication and augments membrane ion currents. *Nat Nanotechnol*. 2018;13:755-764.
13. Kitko KE, Hong T, Lazarenko RM, Ying D, Xu Y-Q, Zhang Q. Membrane cholesterol mediates the cellular effects of monolayer graphene substrates. *Nat Commun*. 2018;9:796.
14. Kim W, Ng JK, Kunitake ME, Conklin BR, Yang P. Interfacing silicon nanowires with mammalian cells. *J Am Chem Soc*. 2007;129(23):7228-7229.
15. Severino FPU, Ban J, Song Q, et al. The role of dimensionality in neuronal network dynamics. *Sci Rep*. 2016;6:29640.
16. Robinson JT, Jorgolli M, Shalek AK, Yoon M-H, Gertner RS, Park H. Vertical nanowire electrode arrays as a scalable platform for intracellular interfacing to neuronal circuits. *Nat Nanotechnol*. 2012;7:180-184.
17. Piret G, Galopin E, Coffinier Y, Boukherroub R, Legrand D, Slomianny C. Culture of mammalian cells on patterned superhydrophilic/superhydrophobic silicon nanowire arrays. *Soft Matter*. 2011;7:8642-8649.
18. Hinde CS, Ansovini D, Wells PP, et al. Elucidating-structure property relationships in the design of metal nanoparticle catalysts for the activation of molecular oxygen. *ACS Catal*. 2015;5:3807-3816.
19. Jin D, Xi P, Wang B, Zhang L, Enderlein J, van Oijen AM. Nanoparticles for super-resolution microscopy and single-molecule tracking. *Nat Methods*. 2018;15:415-423.
20. Parameswaran R, Carvalho-de-Souza JL, Jiang Y, et al. Photoelectrochemical modulation of neuronal activity with free-standing coaxial silicon nanowires. *Nat Nanotechnol*. 2018;13:260-266.
21. Eltom A, Zhong G, Muhammad A. Scaffold techniques and designs in tissue engineering functions and purposes: a review. *Adv Mater Sci Eng*. 2019;2019:3429527.
22. Derakhshanfar S, Mbeleck R, Xu K, Zhang X, Zhong W, Xing M. 3D bioprinting for biomedical devices and tissue

engineering: a review of recent trends and advances. *Bioactive Mater*. 2018;3:144-156.
23. Aldana AA, Abraham GA. Current advances in electrospun gelatin-based scaffolds for tissue engineering applications. *Int J Pharm*. 2017;523:441-453.
24. Kosuge D, Khan WS, Haddad B, Marsh D. Biomaterials and scaffolds in bone and musculoskeletal engineering. *Curr Stem Cell Res Ther*. 2013;8:185-191.
25. Koons GL, Mikos AG. Progress in three-dimensional printing with growth factors. *J Control Release*. 2019;295:50-59.
26. Jiang Y, Tian B. Inorganic semiconductor biointerfaces. *Nat Rev Mater*. 2018;3:473-490.
27. Li S, Huang K, Fan Q, et al. Highly sensitive solution-gated graphene transistors for label-free DNA detection. *Biosens Bioelectron*. 2019;136:91-96.
28. Chen R, Canales A, Anikeeva P. Neural recording and modulation technologies. *Nat Rev Mater*. 2017;2:16093.
29. Koo J, MacEwan MR, Kang S-K, et al. Wireless bioresorbable electronic system enables sustained nonpharmacological neuroregenerative therapy. *Nat Med*. 2018;24(12):1830-1836.
30. Boyden ES, Zhang F, Bamberg E, Nagel G, Deisseroth K. Millisecond-timescale, genetically targeted optical control of neural activity. *Nat Neurosci*. 2005;8:1263-1268.
31. Agostinis P, Berg K, Cengel KA, et al. Photodynamic therapy of cancer: an update. *CA Cancer J Clin*. 2011;61:250-281.
32. Deisseroth K. Optogenetic. *Nat Methods*. 2011;8:26-29.
33. Yizhar O, Fenno LE, Davidson TJ, Mogri M, Deisseroth K. Optogenetics in neural systems. *Neuron*. 2011;71:9-34.
34. Plow EB, Pascual-Leone A, Machado A. Brain stimulation in the treatment of chronic neuropathic and non-cancerous pain. *J Pain*. 2012;13:411-424.
35. Wichmann T, DeLong MR. Deep brain stimulation for neurologic and neuropsychiatric disorders. *Neuron*. 2006;52:197-204.
36. Guniat L, Caroff P, Fontcuberta I, Morral A. Vapor phase growth of semiconductor nanowires: key developments and open questions. *Chem Rev*. 2019;119:8958-8971.
37. Wagner RS, Ellis WC, Wagner RS, Ellis WC. Vapor–liquid-solid mechanism of single crystal growth. *Appl Phy Lett*. 1964;4(5):89-90.
38. Sutter E, Sutter P. Phase diagram of nanoscale alloy particles used for vapor-liquid-solid growth of semiconductor nanowires. *Nano Lett*. 2008;8:411-414.
39. Cahn JW, Carter WC. Crystal shapes and phase equilibria: a common mathematical basis. *MMTA*. 1996;27:1431-1440.
40. Woodruff JH, Ratchford JB, Goldthorpe IA, McIntyre PC, Chidsey CED. Vertically oriented germanium nanowires grown from gold colloids on silicon substrates and subsequent gold removal. *Nano Lett*. 2007;7:1637-1642.
41. Dick KA, Deppert K, Larsson MW, et al. Synthesis of branched 'nanotrees' by controlled seeding of multiple branching events. *Nat Mater*. 2004;3:380-384.
42. Assali S, Dijkstra A, Li A, et al. Growth and optical properties of direct band gap Ge/Ge0.87Sn0.13 core/shell nanowire arrays. *Nano Lett*. 2017;17:1538-1544.
43. Friedl M, Cerveny K, Weigele P, et al. Template-assisted scalable nanowire networks. *Nano Lett*. 2018;18:2666-2671.
44. Gratzel M. Photoelectrochemical cells. *Nature*. 2001;414:338-344.
45. Kim J, Bae S-H, Lim H-G. Micro transfer printing on cellulose electro-active paper. *Smart Mater Struct*. 2006;15:889-892.
46. Lu L, Gutruf P, Xia L, et al. Wireless optoelectronic photometers for monitoring neuronal dynamics in the deep brain. *Proc Natl Acad Sci USA*. 2018;115:E1374-E1383.
47. Rubehn B, Wolff SBE, Tovote P, Luethi A, Stieglitz T. A polymer-based neural microimplant for optogenetic applications: design and first in vivo study. *Lab Chip*. 2013;13:579-588.
48. Park SI, Brenner DS, Shin G, et al. Soft, stretchable, fully implantable miniaturized optoelectronic systems for wireless optogenetics. *Nat Biotechnol*. 2015;33(12):1280-1286.
49. Fu T-M, Hong G, Viveros RD, Zhou T, Lieber CM. Highly scalable multichannel mesh electronics for stable chronic brain electrophysiology. *Proc Natl Acad Sci USA*. 2017;114:E10046-E10055.
50. Liu J, Fu T-M, Cheng Z, et al. Syringe-injectable electronics. *Nature Nanotechnol*. 2015;10:629-636.
51. Kim D-H, Viventi J, Amsden JJ, et al. Dissolvable films of silk fibroin for ultrathin conformal bio-integrated electronics. *Nat Mater*. 2010;9:511-517.
52. Loo YL, Willett RL, Baldwin KW, Rogers JA. Interfacial chemistries for nanoscale transfer printing. *J Am Chem Soc*. 2002;124:7654-7655.
53. Kornev KG, Callegari G, Kuppler J, Ruetsch S, Neimark AV. Ribbon-to-fiber transformation in the process of spinning of carbon-nanotube dispersion. *Phys Rev Lett*. 2006;97:188303.
54. Py C, Reverdy P, Doppler L, Bico J, Roman B, Baroud CN. Capillary origami: spontaneous wrapping of a droplet with an elastic sheet. *Phys Rev Lett*. 2007;98:156103.
55. Xu S, Yan Z, Jang K-I, et al. Assembly of micro/nanomaterials into complex, three-dimensional architectures by compressive buckling. *Science*. 2015;347:154-159.
56. Mei Y, Huang G, Solovev AA, et al. Versatile approach for integrative and functionalized tubes by strain engineering of nanomembranes on polymers. *Adv Mater*. 2008;20:4085-4090.
57. Pandey S, Ewing M, Kunas A, Nghi N, Gracias DH, Menon G. Algorithmic design of self-folding polyhedra. *Proc Natl Acad Sci USA*. 2011;108:19885-19890.
58. Kim J, Hanna JA, Byun M, Santangelo CD, Hayward RC. Designing responsive buckled surfaces by halftone gel lithography. *Science*. 2012;335:1201-1205.
59. Bico J, Roman B, Moulin L, Boudaoud A. Elastocapillary coalescence in wet hair. *Nature*. 2004;432:690-690.
60. Guo X, Li H, Ahn BY, et al. Two- and three-dimensional folding of thin film single-crystalline silicon for photovoltaic power applications. *Proc Natl Acad Sci USA*. 2009;106:20149-20154.
61. Yan Z, Zhang F, Liu F, et al. Mechanical assembly of complex, 3D mesostructures from releasable multilayers of advanced materials. *Sci Adv*. 2016;2(9):e1601014.
62. Zhang Y, Zhang F, Yan Z, et al. Printing, folding and assembly methods for forming 3D mesostructures in advanced materials. *Nat Rev Mater*. 2017;2(4):17019.
63. Lehmhus D, Aumund-Kopp C, Petzoldt F, et al. Customized smartness: a survey on links between additive manufacturing and sensor integration. *Proc Technol*. 2016;26:284-301.
64. Chrisey DB. Materials processing—the power of direct writing. *Science*. 2000;289:879-881.

65. Lewis JA, Gratson GM. Direct writing in three dimensions. *Mater Today*. 2004;7:32-39.
66. Kong YL, Tamargo IA, Kim H, et al. 3D printed quantum dot light-emitting diodes. *Nano Lett*. 2014;14:7017-7023.
67. Ahn BY, Duoss EB, Motala MJ, et al. Omnidirectional printing of flexible, stretchable, and spanning silver microelectrodes. *Science*. 2009;323:1590-1593.
68. Tumbleston JR, Shirvanyants D, Ermoshkin N, et al. Continuous liquid interface production of 3D objects. *Science*. 2015; 347:1349-1352.
69. Kelly BE, Bhattacharya I, Heidari H, Shusteff M, Spadaccini CM, Taylor HKJS. Volumetric additive manufacturing via tomographic reconstruction. *Science*. 2019; 363:1075-1079.
70. Lewis JA. Direct ink writing of 3D functional materials. *Adv Funct Mater*. 2006;16(17):2193-2204.
71. Sirringhaus H, Kawase T, Friend RH, et al. High-resolution inkjet printing of all-polymer transistor circuits. *Science*. 2000; 290:2123-2126.
72. Forrest SR. The path to ubiquitous and low-cost organic electronic appliances on plastic. *Nature*. 2004;428:911-918.
73. Sun Y, Rogers JA. Inorganic semiconductors for flexible electronics. *Adv Mater*. 2007;19:1897-1916.
74. Newbold HG, Google Patents, US3778614A. 1973.
75. Liu Z, Ukida H, Ramuhalli P, Forsyth DS. Integrated imaging and vision techniques for industrial inspection: a special issue on machine vision and applications. *Mach Vis Appl*. 2010;21: 597-599.
76. Tian B, Lieber CM. Synthetic nanoelectronic probes for biological cells and tissues. *Annu Rev Anal Chem*. 2013;6:31-51.
77. Xie C, Liu J, Fu T-M, Dai X, Zhou W, Lieber CM. Three-dimensional macroporous nanoelectronic networks as minimally invasive brain probes. *Nat Mater*. 2015;14:1286-1292.
78. Luo Z, Jiang Y, Myers BD, et al. Atomic gold–enabled three-dimensional lithography for silicon mesostructures. *Science*. 2015;348:1451-1455.
79. Jiang Y, Carvalho-de-Souza JL, Wong RC, et al. Heterogeneous silicon mesostructures for lipid-supported bioelectric interfaces. *Nat Mater*. 2016;15(9):1023-1030.
80. Zhang Y, Yan Z, Nan K, et al. A mechanically driven form of Kirigami as a route to 3D mesostructures in micro/-nanomembranes. *Proc Natl Acad Sci U S A*. 2015;112:11757-11764.
81. Tian B, Cohen-Karni T, Qing Q, Duan X, Xie P, Lieber CM. Three-dimensional, flexible nanoscale field-effect transistors as localized bioprobes. *Science*. 2010;329:830-834.
82. Duan X, Gao R, Xie P, et al. Intracellular recordings of action potentials by an extracellular nanoscale field-effect transistor. *Nat Nanotechnol*. 2012;7(3):174-179.
83. Vargas-Estevez C, Duch M, Duque M, et al. Suspended silicon microphotodiodes for electrochemical and biological applications. *Small*. 2017;13:1701920.
84. Tian B, Xie P, Kempa TJ, Bell DC, CMJNn L. Single-crystalline kinked semiconductor nanowire superstructures. *Nat Nanotechnol*. 2009;4(12):824-829.
85. Lee J, Ozden I, Song Y-K, Nurmikko AV. Transparent intracortical microprobe array for simultaneous spatiotemporal optical stimulation and multichannel electrical recording. *Nat Methods*. 2015;12:1157-1162.
86. Gautam V, Naureen S, Shahid N, et al. Engineering highly interconnected neuronal networks on nanowire scaffolds. *Nano Lett*. 2017;17:3369-3375.
87. Hallstrom W, Martensson T, Prinz C, et al. Gallium phosphide nanowires as a substrate for cultured neurons. *Nano Lett*. 2007;7:2960-2965.
88. Adolfsson K, Persson H, Wallentin J, et al. Fluorescent nanowire heterostructures as a versatile tool for biology applications. *Nano Lett*. 2013;13:4728-4732.
89. Cha C, Shin SR, Annabi N, Dokmeci MR, Khademhosseini A. Carbon-based nanomaterials: multifunctional materials for biomedical engineering. *ACS Nano*. 2013;7:2891-2897.
90. Schwierz F. Graphene transistors. *Nat Nanotechnol*. 2010;5: 487-496.
91. Peng Z, Lin J, Ye R, Samuel ELG, Flexible TJM. Stackable laser-induced graphene supercapacitorse. *ACS Appl Mater Interfaces*. 2015;7:3414-3419.
92. Kostarelos K, Bianco A, Prato M. Promises, facts and challenges for carbon nanotubes in imaging and therapeutics. *Nat Nanotechnol*. 2009;4:627-633.
93. Coleman JN, Khan U, Gun'ko YK. Mechanical reinforcement of polymers using carbon nanotubes. *Adv Mater*. 2006;18:689-706.
94. Correa-Duarte MA, Wagner N, Rojas-Chapana J, Morsczeck C, Thie M, Giersig M. Fabrication and biocompatibility of carbon nanotube-based 3D networks as scaffolds for cell seeding and growth. *Nano Lett*. 2004;4:2233-2236.
95. Abdolahad M, Taghinejad M, Taghinejad H, Janmaleki M, Mohajerzadeh S. A vertically aligned carbon nanotube-based impedance sensing biosensor for rapid and high sensitive detection of cancer cells. *Lab Chip*. 2012;12:1183-1190.
96. Xiao M, Li X, Song Q, et al. A fully 3D interconnected graphene-carbon nanotube web allows the study of glioma infiltration in bioengineered 3D cortex-like networks. *Adv Mater*. 2018;30:1806132.
97. Zhang YB, Tan YW, Stormer HL, Kim P. Experimental observation of the quantum Hall effect and Berry's phase in graphene. *Nature*. 2005;438:201-204.
98. Novoselov KS, Geim AK, Morozov SV, et al. Two-dimensional gas of massless Dirac fermions in graphene. *Nature*. 2005;438: 197-200.
99. Wang Y, Li Z, Wang J, Li J, Lin Y. Graphene and graphene oxide: biofunctionalization and applications in biotechnology. *Trends Biotechnol*. 2011;29:205-212.
100. Hong G, Yang X, Zhou T, Lieber CM. Mesh electronics: a new paradigm for tissue-like brain probes. *Curr Opin Neurobiol*. 2018;50:33-41.
101. Hong G, Viveros RD, Zwang TJ, Yang X, Lieber CM. Tissue-like neural probes for understanding and modulating the brain. *Biochemistry*. 2018;57:3995-4004.
102. Hong G, Fu T-M, Qiao M, et al. A method for single-neuron chronic recording from the retina in awake mice. *Science*. 2018;360:1447-1451.
103. Guan S, Wang J, Gu X, et al. Elastocapillary self-assembled neurotassels for stable neural activity recordings. *Sci Adv*. 2019;5(3):eaav2842.
104. Feiner R, Engel L, Fleischer S, et al. Engineered hybrid cardiac patches with multifunctional electronics for online monitoring and regulation of tissue function. *Nat Mater*. 2016;15: 679-685.

105. Cui X, Wiler J, Dzaman M, Altschuler RA, Martin DCJB. In vivo studies of polypyrrole/peptide coated neural probes. *Biomaterials*. 2003;24:777-787.
106. Kim DH, Richardson-Burns SM, Hendricks JL, Sequera C, Martin DC. Effect of immobilized nerve growth factor on conductive polymers: electrical properties and cellular response. *Adv Funct Mater*. 2007;17(1):79-86.
107. Feiner R, Dvir T. Tissue-electronics interfaces: from implantable devices to engineered tissues. *Nat Rev Mater*. 2018;3(1):17076.
108. Salatino JW, Ludwig KA, Kozai TD, Purcell EK. Glial responses to implanted electrodes in the brain. *Nat Biomed Eng*. 2017;1(11):862-877.
109. Qi D, Liu Z, Liu Y, et al. Highly stretchable, compliant, polymeric microelectrode arrays for in vivo electrophysiological interfacing. *Adv Mater*. 2017;29(40):1702800.
110. Huang J, Lu L, Zhang J, et al. Electrical stimulation to conductive scaffold promotes axonal regeneration and remyelination in a rat model of large nerve defect. *PLoS One*. 2012;7:e39526.
111. Xu H, Holzwarth JM, Yan Y, et al. Conductive PPY/PDLLA conduit for peripheral nerve regeneration. *Biomaterials*. 2014; 35:225-235.
112. Schmidt CE, Shastri VR, Vacanti JP, Langer R. Stimulation of neurite outgrowth using an electrically conducting polymer. *Proc Natl Acad Sci USA*. 1997;94:8948-8953.
113. Wood M, Willits RK. Short-duration, DC electrical stimulation increases chick embryo DRG neurite outgrowth. *Bioelectromagnetics*. 2006;27:328-331.
114. Zimmermann WH, Melnychenko I, Wasmeier G, et al. Engineered heart tissue grafts improve systolic and diastolic function in infarcted rat hearts. *Nat Med*. 2006;12:452-458.
115. Dvir T, Kedem A, Ruvinov E, et al. Prevascularization of cardiac patch on the omentum improves its therapeutic outcome. *Proc Natl Acad Sci USA*. 2009;106:14990-14995.
116. Dvir T, Timko BP, Brigham MD, et al. Nanowired three-dimensional cardiac patches. *Nat Nanotechnol*. 2011;6(11):720-725.
117. Tian B, Liu J, Dvir T, et al. Macroporous nanowire nanoelectronic scaffolds for synthetic tissues. *Nat Mater*. 2012; 11(11):986-994.
118. Dai X, Zhou W, Gao T, Liu J, Lieber CM. Three-dimensional mapping and regulation of action potential propagation in nanoelectronics-innervated tissues. *Nat Nanotechnol*. 2016;11: 776-782.
119. Herron TJ. Optical imaging of voltage and calcium in cardiac cells & tissues. *Circ Res*. 2012;110:609-623.
120. Natarajan A, Stancescu M, Dhir V, et al. Patterned cardiomyocytes on microelectrode arrays as a functional, high information content drug screening platform. *Biomaterials*. 2011; 32:4267-4274.
121. Kim D-H, Lu N, Ghaffari R, et al. Materials for multifunctional balloon catheters with capabilities in cardiac electrophysiological mapping and ablation therapy. *Nat Mater*. 2011;10:316-323.
122. Qing Q, Pal SK, Tian B, et al. Nanowire transistor arrays for mapping neural circuits in acute brain slices. *Proc Natl Acad Sci U S A*. 2010;107:1882-1887.
123. McAlpine MC, Ahmad H, Wang D, Heath JR. Highly ordered nanowire arrays on plastic substrates for ultrasensitive flexible chemical sensors. *Nat Mater*. 2007;6(5):379-384.
124. Wang C, Hwang D, Yu Z, et al. User-interactive electronic skin for instantaneous pressure visualization. *Nat Mater*. 2013;12:899-904.
125. Huang Y, Duan X, Lieber CM. Nanowires for integrated multicolor nanophotonics. *Small*. 2005;1:142-147.
126. Rezwan K, Chen QZ, Blaker JJ, Boccaccini AR. Biodegradable and bioactive porous polymer/inorganic composite scaffolds for bone tissue engineering. *Biomaterials*. 2006;27:3413-3431.
127. Shepherd JNH, Parker ST, Shepherd RF, Gillette MU, Lewis JA, Nuzzo RG. 3D microperiodic hydrogel scaffolds for robust neuronal cultures. *Adv Funct Mater*. 2011;21:47-54.
128. Wan AM-D, Inal S, Williams T, et al. 3D conducting polymer platforms for electrical control of protein conformation and cellular functions. *J Mater Chem B*. 2015;3:5040-5048.
129. Yu M, Huang Y, Ballweg J, et al. Semiconductor nanomembrane tubes: three-dimensional confinement for controlled neurite outgrowth. *ACS Nano*. 2011;5:2447-2457.
130. McCracken JM, Xu S, Badea A, et al. Deterministic integration of biological and soft materials onto 3D microscale cellular frameworks. *Adv Biosyst*. 2017;1(9):1700068.
131. Ramuz M, Tee BCK, Tok JBH, Bao Z. Transparent, optical, pressure-sensitive artificial skin for large-area stretchable electronics. *Adv Mater*. 2012;24:3223-3227.
132. Mannsfeld SCB, Tee BCK, Stoltenberg RM, et al. Highly sensitive flexible pressure sensors with microstructured rubber dielectric layers. *Nat Mater*. 2010;9:859-864.
133. Someya T, Sekitani T, Iba S, Kato Y, Kawaguchi H, Sakurai T. A large-area, flexible pressure sensor matrix with organic field-effect transistors for artificial skin applications. *Proc Natl Acad Sci U S A*. 2004;101:9966-9970.
134. Ho DH, Sun Q, Kim SY, Han JT, Kim DH, Cho JH. Stretchable and multimodal all graphene electronic skin. *Adv Mater*. 2016;28(13):2601-2608.
135. Harada S, Kanao K, Yamamoto Y, Arie T, Akita S, Takei K. Fully printed flexible fingerprint-like three-axis tactile and slip force and temperature sensors for artificial skin. *ACS Nano*. 2014;8:12851-12857.
136. Reeder JT, Kang T, Rains S, Voit W. 3D, reconfigurable, multimodal electronic whiskers via directed air assembly. *Adv Mater*. 2018;30(11):1706733.
137. Abbott J, Ye T, Qin L, et al. CMOS nanoelectrode array for all-electrical intracellular electrophysiological imaging. *Nat Nanotechnol*. 2017;12:460-466.
138. Yang X, Zhou T, Zwang TJ, et al. Bioinspired neuron-like electronics. *Nat Mater*. 2019;18:510-517.
139. Zhang Y, Zheng N, Cao Y, et al. Climbing-inspired twining electrodes using shape memory for peripheral nerve stimulation and recording. *Sci Adv*. 2019;5(4):eaaw1066.
140. Cheng H, Lederer WJ, Cannell MB. Calcium sparks: elementary events underlying excitation-contraction coupling in heart-muscle. *Science*. 1993;262:740-744.
141. Matiukas A, Mitrea BG, Qin M, et al. Near-infrared voltage-sensitive fluorescent dyes optimized for optical mapping in bloodperfused myocardium. *Heart Rhythm*. 2007;4:1441-1451.
142. Hou JH, Kralj JM, Douglass AD, Engert F, Cohen AE. Simultaneous mapping of membrane voltage and calcium in zebrafish heart in vivo reveals chamber-specific developmental transitions in ionic currents. *Front Physiol*. 2014;5:344.

143. Fertig N, Blick RH, Behrends JC. Whole cell patch clamp recording performed on a planar glass chip. *Biophys J*. 2002; 82:3056-3062.
144. Berdondini L, Imfeld K, Maccione A, et al. Active pixel sensor array for high spatio-temporal resolution electrophysiological recordings from single cell to large scale neuronal networks. *Lab Chip*. 2009;9:2644-2651.
145. Frey U, Sedivy J, Heer F, et al. Switch-matrix-based high-density microelectrode array in CMOS technology. *IEEE J Solid-St Circ*. 2010;45:467-482.
146. Wise KD, Angell JB, Starr A. An integrated-circuit approach to extracellular microelectrodes. *IEEE Trans Biomed Eng*. 1970;17(3):238-247.
147. Campbell PK, Jones KE, Normann RA. A 100 electrode intracortical array: structural variability. *Biomed Sci Instrum*. 1990; 26:161-165.
148. Isnard S, Silk WK. Moving with climbing plants from Charles Darwin's time into the 21st century. *Am J Bot*. 2009;96:1205-1221.
149. Sekitani T, Someya T. Stretchable organic integrated circuits for large-area electronic skin surfaces. *MRS Bull*. 2012;37: 236-245.
150. Ordonez J, Schuettler M, Boehler C, Boretius T, Stieglitz T. Thin films and microelectrode arrays for neuroprosthetics. *MRS Bull*. 2012;37:590-598.
151. Sekitani T, Yokota T, Zschieschang U, et al. Organic nonvolatile memory transistors for flexible sensor arrays. *Science*. 2009;326:1516-1519.
152. Borovikova LV, Ivanova S, Zhang MH, et al. Vagus nerve stimulation attenuates the systemic inflammatory response to endotoxin. *Nature*. 2000;405:458-462.
153. Keplinger C, Sun J-Y, Foo CC, Rothemund P, Whitesides GM, Suo Z. Stretchable, transparent, ionic conductors. *Science*. 2013;341:984-987.
154. Liu Y, Liu J, Chen S, et al. Soft and elastic hydrogel-based microelectronics for localized low-voltage neuromodulation. *Nat Biomed Eng*. 2019;3:58-68.
155. Kim T-i, McCall JG, Jung YH, et al. Injectable, cellular-scale optoelectronics with applications for wireless optogenetics. *Science*. 2013;340:211-216.
156. Jiang YW, Li XJ, Liu B, et al. Rational design of silicon structures for optically controlled multiscale biointerfaces. *Nat Biomed Eng*. 2018;2:508-521.
157. Nagel G, Ollig D, Fuhrmann M, et al. Channelrhodopsin-1: a light-gated proton channel in green algae. *Science*. 2002;296: 2395-2398.
158. Balint R, Cassidy NJ, Cartmell SH. Conductive polymers: towards a smart biomaterial for tissue engineering. *Acta Biomater*. 2014;10:2341-2353.
159. Zhou L, Fan L, Yi X, et al. Soft conducting polymer hydrogels cross-linked and doped by tannic acid for spinal cord injury repair. *ACS Nano*. 2018;12:10957-10967.
160. Yamagishi K, Kirino I, Takahashi I, et al. Tissue-adhesive wirelessly powered optoelectronic device for metronomic photodynamic cancer therapy. *Nat Biomed Eng*. 2019;3:27-36.
161. Kim DH, Lu NS, Ghaffari R, Rogers JA. Inorganic semiconductor nanomaterials for flexible and stretchable bio-integrated electronics. *NPG Asia Mater*. 2012;4:e15.

AUTHOR BIOGRAPHIES

Huachun Wang is a PhD candidate in the Department of Electronic Engineering at Tsinghua University, China, under the supervision of Prof Xing Sheng. His current research interests involve design and microfabrication of multiscale optoelectronics for biological applications in tissue engineering and neuroscience. He received his bachelor degree (2014) and master degree (2017) from Nanchang University and Xiamen University, respectively.

Lan Yin is currently working as an associate professor in the School of Materials Science and Engineering at Tsinghua University, China. She received her bachelor and PhD degrees from Tsinghua University and Carnegie Mellon University, respectively. Her current research is focused on biodegradable materials and electronics targeting applications for environment and health care.

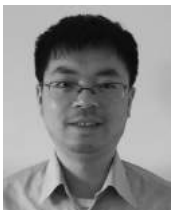

Xing Sheng is currently working as an associate professor in the Department of Electronic Engineering at Tsinghua University, China. He received his bachelor and PhD degrees from Tsinghua University and Massachusetts Institute of Technology, respectively. His current research is focused on advanced optoelectronic materials, devices, and systems for biomedical applications.

How to cite this article: Wang H, Sun P, Yin L, Sheng X. 3D electronic and photonic structures as active biological interfaces. *InfoMat*. 2020;2: 527–552. https://doi.org/10.1002/inf2.12054